Energy-Dependent Pion-Nucleon Phase-Shift Analysis*†

L. DAVID ROPER AND ROBERT M. WRIGHT
Lawrence Radiation Laboratory, University of California, Livermore, California

AND

BERNARD T. FELD
Physics Department and Laboratory for Nuclear Science, Massachusetts Institute of Technology, Cambridge, Massachusetts

(Received 23 November 1964)

Energy-dependent pion-nucleon phase-shift analyses have been carried out in the energy ranges 0–50, 0–100, 0–350, 0–700, and 300–800 MeV. An outline of the procedure is given. The results obtained with all available data are presented. The best solution in the 0–350-MeV range is obtained by starting from Donnachie, Hamilton, and Lea's predicted phases, although the final results differ widely from the input. The best solution obtained in the 0–700-MeV range contains three resonances: in the P_{33} state at 193 MeV, the P_{11} state at approximately 585 MeV, and the D_{13} state at 638 MeV. The last two are strongly absorptive. A good solution has been obtained without the P_{11} phase shift actually going through 90°, but it must be large (about 80°) at 700 MeV. The 0–100-, the 0–350-, and the 0–700-MeV solutions are consistent with each other in the large phases. The P_{11}, P_{13}, and P_{31} phases cannot be precisely determined by using only the 0–50-MeV data.

I. INTRODUCTION

IN recent years evidence has been accumulating that the pion-nucleon interaction cannot be adequately represented by single dominating angular-momentum states in the vicinities of the prominent bumps in the total cross sections higher in energy than the first (the P_{33} resonance[1] which appears at about 200-MeV pion laboratory kinetic energy). This has led to a multitude of theoretical schemes to explain the higher energy scattering.

If one is to compare any of these complicated schemes with experiment, some common meeting ground must be achieved between the large quantity of experimental data and the proposed theories. Traditionally this meeting ground has resulted from an analysis of the data in terms of phase shifts. A passing glance at the phase shifts reported at single energies immediately tells one that they provide a poor meeting ground because of the complete lack of uniqueness.[2] This unpleasant situation has led us to attempt to obtain phase shifts as functions of energy by considering simultaneously all the data in the energy range of interest; it was hoped, thereby, that a unique solution might be obtained or, at least, that the scatter among different solutions would be reduced.

Since pion-nucleon scattering data of many kinds are very plentiful over a wide range of energies, and new measurements are being made at a rapid rate, it seems reasonable to expect to succeed in obtaining a unique set of energy-dependent phase shifts over the energy ranges in which the prominent features occur. The main objective of the investigation reported here was to set up a computer program in which one could insert expressions embodying any desired functions of energy for the phase shifts and absorption parameters (or for the real and imaginary parts of the partial-wave amplitudes) and then vary any number of parameters in the functions to fit all of the data. In choosing the method of parametrization, our criteria were that it should involve only the most general theoretical assumptions and be a form of sufficient flexibility to be capable of representing many kinds of phase-shift behavior, excluding only the most extreme.

We have attempted such an energy-dependent analysis for the energy ranges 0–50, 0–100, 0–350, 0–700, and 300–800 MeV. One 0–700-MeV solution has been obtained that gives a better fit to the data than any other solution investigated. The outstanding features of this solution are:

(1) Resonances occur in the P_{33} state at 193 MeV, the P_{11} state at about 585 MeV,[3] and the D_{13} state at 638 MeV. (The total c.m. energies are, respectively, 1234, 1503, and 1536 MeV.)

(2) The F_{15} phase shift becomes greater than the D_{15} phase shift at about 585 MeV and is apparently headed towards dominance at 900 MeV. (A preliminary analysis of the 0–1100-MeV range favors this conjecture.)

(3) There is strong absorption in the P_{11}, D_{13}, S_{11}, and P_{31} states.

The P_{11} resonance we find at about 585 MeV does not fit on any known Regge trajectory, nor does it fit into any established $SU(3)$ octet. It has the same

* Work performed under the auspices of the U. S. Atomic Energy Commission.

† Based in part on a thesis presented by L. David Roper to the Massachusetts Institute of Technology in partial fulfillment of the requirements for the degree of Doctor of Philosophy.

[1] We use the usual notation for the nucleon-pion states, $l_{2T,2J}$.

[2] J. M. McKinley, Rev. Mod. Phys. 35, 788 (1963).

[3] L. D. Roper, Phys. Rev. Letters 12, 340 (1964).

quantum numbers as the nucleon, but a higher mass (by around 565 MeV). We have made many efforts, with no success to date, to find a solution without a large P_{11} phase shift that adequately fits the data. Solutions have been obtained without a P_{11} resonance, but the fits are not as good as when the P_{11} resonates. Even in these solutions the P_{11} phase is large at 700 MeV (approximately 80°).

This P_{11} resonance and the nearby D_{13} resonance are both highly absorptive. Owing to the fact that the D_{13} partial-wave amplitude is multiplied by a factor of 2 in the expression for the total cross section as compared to the P_{11} amplitude,[4] the total cross-section bump at approximately 600 MeV is predominantly caused by the D_{13} resonance but with a low-energy asymmetry due to the P_{11} resonance.[5]

Other analyses similar in philosophy to this one are underway at Yale[6] and at the Rutherford Laboratory.[7] The Yale analysis covers the 0–350-MeV range, and the results obtained are similar to our 0–350-MeV results. Both the Yale and Rutherford analyses use parametrizations developed by means of partial-wave dispersion relations.

Auvil and Lovelace[8] have reanalyzed available differential cross sections in terms of Legendre polynomial series and have been able to extract much information from the coefficients thus obtained. They obtain some more information about the partial-wave amplitudes by requiring "that the elasticities of the resonances, as determined from total cross sections and forward dispersion relations, be compatible with the differential cross sections." However, they do not fully utilize the polarization data.

The equations relating the observables to the partial-wave amplitudes for π-N scattering are given in Appendix I. Appendix II contains pion-nucleon scattering data references. In Sec. II we describe how we take account of electromagnetic effects. The energy dependence and procedure used in this analysis are given in Sec. III, and Sec. IV contains a short discussion of the available data. Section V is devoted to a brief description of the computer code (PIP) used in the analysis. The 0–350-MeV results are in Sec. VI, the 0–700- and 300–800-MeV results are in Sec. VII, and the 0–50- and 0–100-MeV results are in Sec. VIII.

II. ELECTROMAGNETIC EFFECTS

Our notation for the phase shifts and amplitudes, in terms of which we compute cross sections and polarizations, is given in Appendix I.

To account for electromagnetic effects in $\pi^{\pm}+p\rightarrow$ $\pi^{\pm}+p$ scattering, we use the method of Foote *et al.*[9] with the following changes: (1) Our expressions for the amplitudes are fully relativistic, although correct relativistically only to first order in α, the fine structure constant. We use these amplitudes rather than the amplitudes used by Foote *et al.* which are correct only to second order in $\beta_p=k/p_0$ where k is the pion c.m. momentum and $p_0=(k^2+M^2)^{1/2}$ is the proton total c.m. energy.[10] (2) No attempt is made to preserve unitarity for the relativistic corrections. (The addition of the relativistic correction parts of the electromagnetic amplitudes causes unitarity to be violated, but only slightly so except at very low energies.)

The relativistic electromagnetic amplitudes, to first order in α,[11] are

$$f_{\mathrm{rem}}^{\pm}(\theta)=\frac{\mp\alpha\lambda}{2W(1-\cos\theta)}\left[\frac{W-M}{p_0-M}+\frac{W+M}{p_0+M}\cos\theta-(u_p-1)\frac{q_0}{M}(1-\cos\theta)-(\mu_p-1)\frac{p_0-M}{2M}\sin^2\theta\right], \quad (1)$$

$$g_{\mathrm{rem}}^{\pm}(\theta)=\frac{\pm\alpha\lambda\sin\theta}{2W(1-\cos\theta)}\left[\frac{W+M}{p_0+M}+(\mu_p-1)\frac{W+q_0+M}{2M}+(\mu_p-1)\frac{p_0-M}{2M}\cos\theta\right],$$

where the pion total c.m. energy is $q_0=(k^2+1)^{1/2}$, the total energy is $W=p_0+q_0$, θ is the c.m. pion scattering angle, $M=6.7212$ is the proton mass, $\lambda=1.4135\times10^{-13}$ cm is the pion Compton wavelength, and $\mu_p=2.79275$ is the proton magnetic moment in nuclear magnetons. These equations agree with Solmitz's[12] equations in the approximation that Solmitz uses. The nonrelativistic electromagnetic (Coulomb) amplitudes, correct to all orders in α, are[13]

$$f_{\mathrm{Coul}}^{\pm}(\theta)=\frac{\mp\alpha\lambda(q_0p_0+k^2)}{k^2W(1-\cos\theta)}\exp\left[\mp i\frac{\alpha(q_0p_0+k^2)}{kW}\times\ln\left(\frac{1-\cos\theta}{2}\right)\right], \quad (2)$$

$$g_{\mathrm{Coul}}^{\pm}(\theta)=0.$$

[4] See Appendix I.

[5] P. Bareyre, C. Bricman, G. Valladas, G. Villet, J. Bizard, and J. Sequinot, Phys. Letters 8, 137 (1964).

[6] F. Lin, Yale University (private communication).

[7] R. G. Moorhouse, Rutherford High Energy Laboratory (private communication); B. H. Bransden, P. J. O'Donnell, and R. G. Moorhouse, Phys. Letters 11, 339 (1964).

[8] P. Auvil and C. Lovelace, Nuovo Cimento 33, 473 (1964).

[9] J. H. Foote, O. Chamberlain, E. H. Rogers, and H. M. Steiner, Phys. Rev. 122, 959 (1961).

[10] All masses, energies, and momenta are in units of the pion mass, $\mu=139.59$ MeV.

[11] L. D. Roper, Ph.D. thesis, Massachusetts Institute of Technology, 1963 (unpublished).

[12] F. T. Solmitz, Phys. Rev. 94, 1799 (L) (1954).

[13] L. I. Schiff, *Quantum Mechanics* (McGraw-Hill Book Company, Inc., New York, 1949); C. L. Critchfield and D. C. Dodder, Phys. Rev. 76, 602 (1949); L. Van Hove, Phys. Rev. 88, 1358 (1952).

[The kinematic factors in $f_{\text{Coul}}{}^{\pm}(\theta)$ reduce to the usual ones in the nonrelativistic limit.] These amplitudes are obtained by solving Schrödinger's equation with a Coulomb potential. To first order in α the Coulomb amplitudes are

$$f_{\text{Coul}\alpha}{}^{\pm}(\theta)=\frac{\mp\alpha\lambda(q_0p_0+k^2)}{k^2W(1-\cos\theta)}, \qquad (3)$$

$$g_{\text{Coul}\alpha}{}^{\pm}(\theta)=0.$$

Taking the nonrelativistic limit of the relativistic amplitudes [Eq. (1)] yields the same amplitudes given in Eq. (3), as it should. Thus, electromagnetic amplitudes, correct nonrelativistically to all orders in α and relativistically to first order in α, can be obtained by subtracting Eq. (3) from the sums of Eqs. (1) and (2):

$$f_{\text{em}}{}^{\pm}(\theta)=f_{\text{rem}}{}^{\pm}(\theta)+f_{\text{Coul}}{}^{\pm}(\theta)-f_{\text{Coul}\alpha}{}^{\pm}(\theta)$$

and

$$g_{\text{em}}{}^{\pm}(\theta)=g_{\text{rem}}{}^{\pm}(\theta)+g_{\text{Coul}}{}^{\pm}(\theta)-g_{\text{Coul}\alpha}{}^{\pm}(\theta)=g_{\text{rem}}{}^{\pm}(\theta).$$

These are the electromagnetic amplitudes used in this work.

The total amplitudes for $\pi^{\pm}+p\rightarrow\pi^{\pm}+p$ scattering are now

$$f^{\pm}(\theta)=f_N{}^{\pm}(\theta)+f_{\text{em}}{}^{\pm}(\theta)$$

and

$$g^{\pm}(\theta)=g_N{}^{\pm}(\theta)+g_{\text{em}}{}^{\pm}(\theta).$$

The pion-nucleon amplitudes (subscript N) modified to include the Coulomb phase shifts Φ_l are[13]:

$$f_N{}^{\pm}(\theta)=\frac{\lambda}{k}\sum_{l=0}^{l_m}e^{\pm2i\Phi_l}[(l+1)A_{l+}{}^{\pm}+lA_{l-}{}^{\pm}]P_l(\cos\theta)$$

and

$$g_N{}^{\pm}(\theta)=\frac{\lambda}{k}\sum_{l=0}^{l_m}e^{\pm2i\Phi_l}[A_{l+}{}^{\pm}-A_{l-}{}^{\pm}]P_l{}^1(\cos\theta),$$

where

$$\Phi_l=\sum_{n=1}^{l}\tan^{-1}\left[\frac{\alpha(q_0p_0+k^2)}{kWn}\right]$$

for $l>0(\Phi_0=0)$.

For charge-exchange scattering we follow the method used by Vik and Rugge[14] (cf. Sorenson's work[15]) in which a Coulomb phase shift of one-half of the $\pi^-+p\rightarrow\pi^-+p$ phase shift is used. There are no electromagnetic amplitudes. Thus, for the charge-exchange amplitudes we use

$$f^{\text{cx}}(\theta)=f_N{}^{\text{cx}}(\theta)=\frac{\lambda}{k}\sum_{l=0}^{l_m}e^{-i\Phi_l}[(l+1)A_{l+}{}^{\text{cx}}+lA_{l-}{}^{\text{cx}}]P_l(\cos\theta)$$

and

$$g^{\text{cx}}(\theta)=g_N{}^{\text{cx}}(\theta)=\frac{\lambda}{k}\sum_{l=0}^{l_m}e^{-i\Phi_l}[A_{l+}{}^{\text{cx}}-A_{l-}{}^{\text{cx}}]P_l{}^1(\cos\theta).$$

[14] O. T. Vik and H. R. Rugge, Phys. Rev. **129**, 2311 (1963).
[15] R. A. Sorenson, Phys. Rev. **112**, 1813 (1958).

Equations (3) provide the bulk of the electromagnetic effects. The other equations represent very minute corrections.

III. PARAMETRIZATION OF PARTIAL-WAVE AMPLITUDES

Rather than do single energy phase-shift analyses and then try to connect the single energy phases smoothly as functions of energy, we chose to parametrize the phase shifts and absorption parameters as functions of energy with variable parameters. The computer code is set up so that many types of energy-dependent forms can be easily inserted. As a first try we chose the following parametrization:

$$A_{l\pm}{}^{(2T)}=\epsilon A_{l\pm}{}^{(2T)}(\text{res})+A_{l\pm}{}^{(2T)}(\text{nonres}),$$

where

$$A_{l\pm}{}^{(2T)}(\text{res})=\frac{-\frac{1}{2}\Gamma_{\text{el}l\pm}{}^{(2T)}}{(q_0-q_{0l\pm}{}^{(2T)})+\frac{1}{2}i\Gamma_{tl\pm}{}^{(2T)}}$$

is the resonance amplitude;

$$A_{l\pm}{}^{(2T)}(\text{nonres})=\frac{1}{2i}(\bar{\eta}_{l\pm}{}^{(2T)}e^{2i\bar{\delta}_{l\pm}{}^{(2T)}}-1)$$

is the amplitude for states in which there are no resonances ($\epsilon=0$) or is the background for resonant states ($\epsilon=1$);

$$\Gamma_{\text{el}l\pm}{}^{(2T)}=\frac{4M}{q_0+q_{0l\pm}{}^{(2T)}}kr_{0l\pm}{}^{(2T)}(\gamma_{l\pm}{}^{(2T)})^2V_l(kr_{0l\pm}{}^{(2T)})$$

is the resonance elastic width (the Layson resonance form[16]);

$$V_l(kr_{0l\pm}{}^{(2T)})=1/[k^2(r_{0l\pm}{}^{(2T)})^2][j_l^2(kr_{0l\pm}{}^{(2T)})+n_l^2(kr_{0l\pm}{}^{(2T)})]$$

is the barrier penetration factor[16];

$$\Gamma_{tl\pm}{}^{(2T)}=\Gamma_{\text{el}l\pm}{}^{(2T)}+\Gamma_{\text{in}l\pm}{}^{(2T)},$$

is the resonance total width;

$$\Gamma_{\text{in}l\pm}{}^{(2T)}=\bar{\Gamma}_{\text{in}l\pm}{}^{(2T)}(k-k_0)^{2l+1},$$

is the resonance inelastic width;

k_0 = threshold pion c.m. momentum for one-pion production = 1.479,

$q_0=(1+k^2)^{1/2}$ = total pion c.m. energy,

$q_{0l\pm}{}^{(2T)}$ = resonance position (sometimes denoted by q_{0r}),

$\epsilon=1$ for states in which we choose to put a resonance,

$\epsilon=0$ for states in which we do not put a resonance,

$$\tan\bar{\delta}_{l\pm}{}^{(2T)}=k^{2l+1}\sum_{n=0}^{l_m-l}[a_{l\pm}{}^{(2T)}]_nk^n \qquad (4)$$

[16] W. M. Layson, Nuovo Cimento **27**, 724 (1963). Equation (4.4) should have γ^2 in it rather than γ.

or

$$\bar{\delta}_{l\pm}{}^{(2T)}=k^{2l+1}\sum_{n=0}^{l_m-l}[a_{l\pm}{}^{(2T)}]_n k^n, \qquad (5)$$

$$\bar{\eta}_{l\pm}{}^{(2T)}=e^{-2\nu},$$

and

$$\nu=0 \quad \text{for} \quad k<k_0,$$

$$\nu=(k-k_0)^{2l+1}\sum_{n=0}^{l_m-l}[b_{l\pm}{}^{(2T)}]_n(k-k_0)^n \quad \text{for} \quad k\gtrsim k_0.$$

(The subscripts and superscripts have been suppressed on ν.) Thus the correct threshold behavior is guaranteed for the phase shifts and approximated for the absorption parameters. The number of a parameters is $2(l_m+1)^2$, and the number of b parameters is $2(l_m+1)^2$.

The actual phase shifts and absorption parameters are

$$\delta_{l\pm}{}^{(2T)}=\tfrac{1}{2}\tan^{-1}\left[\frac{2\,\mathrm{Re}A_{l\pm}{}^{(2T)}}{1-2\,\mathrm{Im}A_{l\pm}{}^{(2T)}}\right]$$

and

$$\eta_{l\pm}{}^{(2T)}=2[(\mathrm{Re}A_{l\pm}{}^{(2T)})^2+(\tfrac{1}{2}-\mathrm{Im}A_{l\pm}{}^{(2T)})^2]^{1/2}.$$

In the case of $\epsilon=0$ these expressions are redundant. In order that unitarity be preserved, we make the restrictions:

$$-\tfrac{1}{2}\leq\mathrm{Re}A_{l\pm}{}^{(2T)}\leq\tfrac{1}{2},$$
$$0\leq\mathrm{Im}A_{l\pm}{}^{(2T)}\leq 1,$$

and

$$0\leq\eta_{l\pm}{}^{(2T)}\leq 1.$$

These first two restrictions are necessary only when $\epsilon=1$; i.e., when a resonance is put in a state and a background is present. The last restriction is equivalent to $\nu_{l\pm}{}^{(2T)}\geq 0$.

The reduced elastic width $(\gamma_{l\pm}{}^{(2T)})^2$ and the interaction range $r_{0_{l\pm}}{}^{(2T)}$ could possibly be different for different states that resonate. However, for simplicity, we initially fixed them at the values given by Layson,[16] $(\gamma_{l\pm}{}^{(2T)})^2=0.133$ and $r_{0_{l\pm}}{}^{(2T)}=0.71$. Later we allowed $(\gamma_{l\pm}{}^{(2T)})^2$ to vary for each resonant state.

It may be that our method of providing the nonresonant background to a resonance is not a good one. It would probably be better to use

$$A_{l\pm}{}^{(2T)}=A_{l\pm}{}^{(2T)}(\text{nonres})+\epsilon\bar{\eta}_{l\pm}{}^{(2T)}(\exp 2i\bar{\delta}_{l\pm}{}^{(2T)})\times A_{l\pm}{}^{(2T)}(\text{res})$$
$$=A_{l\pm}{}^{(2T)}(\text{nonres})+\epsilon A_{l\pm}{}^{(2T)}(\text{res})\times[1+2iA_{l\pm}{}^{(2T)}(\text{nonres})]$$

instead of the parametrization given above. With this parametrization unitarity is automatically preserved as long as $0\leq\bar{\eta}_{l\pm}{}^{(2T)}\leq 1$. We plan to use this method soon.

For the 0–350-MeV analysis we used as input values for the coefficients of the lowest powers of k (scattering lengths) in the $\tan\bar{\delta}$ energy-dependent form, Eq. (4), the values given by Hamilton and Woolcock,[17] except for the P_{33} phase shift which was made resonant. The input values are

$$[a_0{}^{(1)}]_0=0.171, \qquad [a_0{}^{(3)}]_0=-0.088,$$
$$[a_{1-}{}^{(1)}]_0=-0.101, \qquad [a_{1-}{}^{(3)}]_0=-0.038,$$

and

$$[a_{1+}{}^{(1)}]_0=-0.029.$$

The 0–350-MeV analysis has been done with the scattering lengths fixed at the Hamilton-Woolcock values and, also, with them allowed to vary. All other a coefficients and the b coefficients were started at zero. A 0–350-MeV analysis was also done in which *all* a and b coefficients were started at zero. The analysis starting from the Hamilton-Woolcock values yielded the best solution; however, the large phases are practically the same in both cases. Later we tried other input. (See Sec. VI.)

The Hamilton-Woolcock 0–350-MeV solution was used as input for the 0–700-MeV analysis. Equation (4) was used for $\bar{\delta}$ until it became obvious that the P_{11} phase is large; then the parametrization of Eq. (5) was used to permit the phase to go through 90° if the data so dictated. (Since the P_{11} phase did go through 90°, a resonance form for the phase shift was put in for the P_{11} that allowed a negative phase shift at low energies, and a slightly better fit was obtained.[3] However, the Layson resonance form for the amplitude did not yield a good fit until it was modified to give the elastic width a zero.) Actually, first the 0–700-MeV total cross sections were fitted starting from the 0–350-MeV solution in order to minimize the renormalization of the differential-cross-section data in the calculation using all of the data. (See Sec. V.) Resonances were tried in several states at $\approx$600 MeV.

Following the suggestion of several people, we did a few 300–800-MeV calculations. The object was to see if the Layson resonance form could be used for the P_{11} state when the lower energy data are excluded. It was found that the Layson form gives a fit comparable to that obtained when the parametrization of Eq. (5) is used, but that the resonance position is considerably higher.

After completion of the 0–350- and 0–700-MeV analyses, 0–50- and 0–100-MeV analyses were undertaken, starting from Hamilton-Woolcock scattering lengths and from zero scattering lengths.

IV. DATA

The data that are available are the total cross sections $\sigma_T{}^+$ and $\sigma_T{}^-$; the elastic and charge-exchange differential cross sections $\sigma^+(\theta)$, $\sigma^-(\theta)$, and $\sigma^{ex}(\theta)$; and the recoil-nucleon polarizations $P^+(\theta)$, $P^-(\theta)$, and $P^{ex}(\theta)$.

[17] J. Hamilton and W. S. Woolcock, Rev. Mod. Phys. 35, 737 (1963).

TABLE I. Energies at which recoil-nucleon polarization data and charge-exchange differential-cross-section data are available. The number of data at each energy and the c.m. pion scattering angles or angular intervals are given. The data reference number (or numbers) is enclosed in parenthesis after each entry in the table.

E_π (MeV)	$\sigma^{cx}(\theta)$	$P^+(\theta)$	$P^-(\theta)$	$P^{cx}(\theta)$
31	3 LPC[a] (B70)			
40	3 CC[b] (B14)			
61	3 LPC (B52)			
65	3 CC (B12)			
95	3 LPC (B52)			
96.6	3 CC (B81)			
120	3 CC (B4)			
128	3 LPC (B58)			
135	3 CC (B1)			
144	3 CC (B4)			
150	3 CC (B23)			
150	3 CC (B51)			
165	3 CC (B19)			
169	3 CC (B7)			
170	3 CC (B23)			
187	3 CC (B20)			
194	3 CC (B7)			
210	3 CC (B7)			
217	3 CC (B13)			
220	3 CC (B30)			
224			2(111°, 146°) (C1)	
230	3 LPC (B59)			
240	3 LPC (B58)			
246		7(68°–147°) (C9)		
260	3 LPC (B59)			
270	3 LPC (B58)			
290	3 LPC (B59)			
300			4(114°–141°) (C3)	
307	3 LPC (B58)	1(140°) (C2)		
310		4(114°–145°) (C4)	4(114°–145°) (C6)	1(30°) (C7)
313	11(58°–159°) (B91)			
317	3 LPC (B59, 91)			
333	3 LPC (B58)			
371	3 LPC (B59, 91)			
371	6(49°–97°), 6(57°–159°) (B91)			
500			3(75°–135°) (C5)	
523		9(76°–139°) (C8)	10(76°–142°) (C8)	
533	20(18°–162°) (B88)			
572		10(73°–139°) (C8)	11(73°–142°) (C8)	
581	20(18°–162°) (B88)			
616			2(85°, 135°) (C5)	
650	20(18°–162°) (B88)			
667			1(120°) (C5)	
689		9(69°–135°) (C8)	11(70°–139°) (C8)	
698	20(18°–162°) (B88)			
Totals	190 data 33 energies	40 data 6 energies	48 data 9 energies	1 datum 1 energy

[a] Legendre polynomial series coefficients.
[b] Cosθ series coefficients.

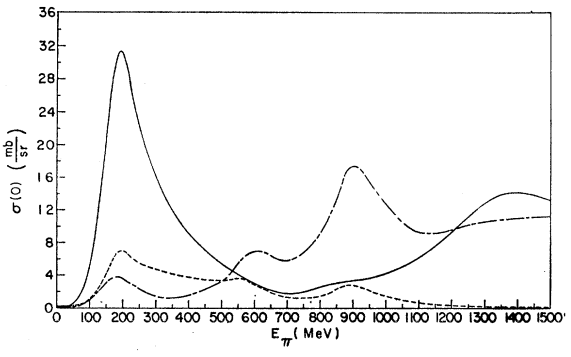

FIG. 1. Forward π^+ elastic (solid), π^- elastic (long dash), and charge-exchange (short dash) differential cross sections as calculated from Niederer's (Ref. 21) forward-amplitude dispersion relation preliminary calculations.

[Only one measurement of $P^{cx}(\theta)$ is presently available.[18]] No measurements have been made of the spin-rotation parameters,[19] $A(\theta)$ and $R(\theta)$. Equations relating these observables to the phase shifts are given in Appendix I. References for the various kinds of data are given in Appendix II.

One can treat the real part of the forward scattering amplitude at a given energy as a datum since it is calculated from the dispersion-relation integral over total cross sections at all energies. Cronin[20] and, more

[18] R. E. Hill, N. E. Booth, R. J. Esterling, D. L. Jenkins, N. H. Lipman, H. R. Rugge, and O. T. Vik, Bull. Am. Phys. Soc. **9**, 410 (A) (1964).
[19] Y. S. Kim, Phys. Rev. **129**, 862 (1963).
[20] J. W. Cronin, Phys. Rev. **118**, 824 (1960).

recently, Niederer,[21] Höhler,[22] and Cence *et al.*[23] have independently made the necessary calculations. We use Niederer's preliminary results. Actually, we use the forward-scattering differential cross section rather than the real part of the amplitude[24] (see Fig. 1). The equations relating them are

$$\sigma^{\pm}(0)=[\mathrm{Re}f^{\pm}(0)]^2+\left[\frac{k}{4\pi\lambda}\sigma_T{}^{\pm}\right]^2$$

and

$$\sigma^{\mathrm{ex}}(0)=\tfrac{1}{2}[\mathrm{Re}f^{+}(0)-\mathrm{Re}f^{-}(0)]^2+\frac{1}{2}\left[\frac{k}{4\pi\lambda}(\sigma_T{}^{+}-\sigma_T{}^{-})\right]^2.$$

Values of these "data" were included at approximately 30-MeV intervals. Initially a large error of 3 mb/s was used in the least-squares fitting at all energies, but the final solution falls well inside this error. Later an error of 1 mb/s was used.

Precise values of the total cross sections and the differential cross sections for elastic scattering are available at many energies in the 0–700-MeV energy range. Table I lists the energies at which $\sigma^{\mathrm{ex}}(\theta)$ and recoil-nucleon polarization data are available.

We have leaned heavily upon the work of Klepikov *et al.*[25] from Dubna in obtaining the total cross-section values. This Dubna work contains almost all of the total cross sections available in March 1960. Several corrections to the original data were made by them, including "Coulomb corrections."

We renormalized a few of the older differential-cross-section data so that the corresponding elastic cross sections are more in conformity with the large body of data. Initially only those data were rejected whose original authors had later repudiated or given corrected versions. Owing to lack of computer memory storage and computer running time, we later found it necessary to lay aside some of the older data at energies where new, more precise, measurements are available. We did not, however, discard data merely because of inconsistencies with other data; thus, our χ^2's are necessarily high.

Only the most recent charge-exchange differential cross section data are obtainable in terms of measured values at each angle. The earlier data are given as coefficients of power series in $\cos\theta$, coefficients of Legendre polynomial series, values of the gamma-ray production differential cross section at each angle, or some combination of these. The relevant equations connecting these quantities to the phase shifts have been given elsewhere.[26]

Regarding recoil-nucleon polarization the main consideration is to maintain a fixed reference direction for the polarization. We adopt the usual direction, namely, $\hat{n}=\mathbf{k}\times\mathbf{k}'/|\mathbf{k}\times\mathbf{k}'|$. All of the data have been given in terms of this direction except that of recoil-nucleon polarization reference C1 (Appendix II), which used $-\hat{n}$. It was necessary to convert the angles from the laboratory system to the c.m. system for the data of Refs. C1 and C3.

Inelastic cross sections were not used in this analysis, however, the agreement of our solution's prediction with the data is good.[26] We have altered the computer code to allow their use.

V. COMPUTATION PROCEDURE

The purpose is to fit the experimental data by adjusting the variable parameters in the theoretical expressions. The usual measure of fit is the quantity χ^2 of the method of least squares.[27] This quantity is defined as the sum, over all the data, of the squares of the deviations of computed values from experimental values of the data, measured in terms of the experimental standard errors. Those values of the variable parameters are sought which minimize χ^2.

There are two types of parameters: those which enter nonlinearly into the expressions used to compute the measured quantities, and those which appear linearly. The parameters associated with the partial-wave amplitudes are of the first type, for which the χ^2-minimizing values must be found by some approximation method. The second type of parameter is represented by the absolute normalization factors associated with differential-cross-section data, i.e., an angle-independent uncertainty is introduced by the uncertainty in the incident beam flux. The χ^2-minimizing values of these parameters may be solved for exactly (for given values of the nonlinear parameters).

The approximation method used to find the desired values of the nonlinear parameters reported in this paper is a modified grid search developed by Arndt and one of the authors (R.M.W.). A grid search consists of the variation of parameters one at a time, recalculating χ^2 for each variation. Each parameter is varied by arbitrarily chosen increments in the appropriate direction until the greatest decrease in χ^2 is found. The modification consists of finding three-parameter values which bracket the best value, and using an interpolating parabola fit to those points to approximate the best

[21] J. Niederer, University of Pennsylvania (private communication).
[22] G. Höhler, Karlsruhe, Germany (private communication).
[23] R. J. Cence, D. A. Cheng, and C. B. Chiu, Lawrence Radiation Laboratory, Berkeley, California (private communication).
[24] It has been pointed out that fitting to the forward cross section is not as sensitive to the forward dispersion-relation calculation as is fitting to the real part of the forward amplitude (Ref. 23). We have recently included the real part of the forward amplitude as data at intervals of 20 MeV, and are able to fit it quite well.
[25] N. P. Klepikov, V. A. Meshcheryakov, and S. N. Sokolov, Joint Institute of Nuclear Research Report JINR-D-584, 1960 (unpublished).
[26] L. D. Roper and R. M. Wright, Lawrence Radiation Laboratory (Livermore) Report UCRL-7846 (1964).
[27] J. Orear, Lawrence Radiation Laboratory (Berkeley) Report UCRL-8417, 1958 (unpublished); P. Cziffra and M. J. Moravcsik, Lawrence Radiation Laboratory (Berkeley) Report UCRL-8523 Rev., 1959 (unpublished).

TABLE II. The characteristics of some of the 0–350-MeV calculations. $E_{\pi r}$ is the P_{33} resonance position in terms of the pion laboratory kinetic energy.

Solution	No. of data	l_m	Absorption	Scattering lengths fixed	Special features[a]	$E_{\pi r}$ (MeV)	Tanδ param.	No. of normalization parameters	χ^2_{norm}	No. of parameters	Expected χ^2	χ^2	χ^2/χ^2_{exp}
1	576	1		×	Started from HW s.l. and P_{33} res.	193	All phases			16	560	2794	4.99
2	576	1		×	Renormalization added to 1	193	All	59	141	16	560	2128	3.80
3	576	1			Started from solution 2	193	All	59	163	21	555	1965	3.54
4	576	2		×	Started from HW s.l. and P_{33} res.	193	All			14	562	2072	3.69
5	576	2		×	Renormalization added to 4	193	All	59	159	14	562	1271	2.26
6	576	2		×	Started from HW s.l. and P_{33} res.	193	All	59	142	14	562	1277	2.27
7	576	2		×	More parameters added to sol. 6	193	All	59		56	520	1249	2.40
8	576	2			Started from sol. 6	193	All	59	144	19	557	1209	2.17
9	576	2	×		Started from sol. 6	193	All	59	156	32	544	1147	2.11
10	576	2			Started from sol. 6	193	None	59	132	19	557	1216	2.18
11	576	2		×	Finkler form[b] for P_{33} Started from sol. 6	193	All	59	127	16	560	1200	2.14
12	576	2			Started from zero s.l. and P_{33} res.	193	All	59	118	19	557	1359	2.44
13	576	2		×	Started from HW s.l. and P_{33} res.	193	None	59	212	14	562	1701	3.03
14	962	2		×	Started from sol. 6	193	All	103	255	14	948	2372	2.50
15	576	3			Started from sol. 12	193	All	59	110	33	543	1043	1.92
16	576	3		×	Started from sol. 6	193	All	59	151	28	548	1091	1.99
17	915	3			Started from HW s.l. and P_{33} res.	193	All		244	33	882	1734	1.97
18	576	3	×		Started from sol. 17	193	All	59	135	65	511	973	1.90[c]
19	576	3	×		Started from HW s.l. and P_{33} res.	193	All			65	511	1524	2.98
20	576	3	×		Renormalization added to 19	193	All	59	113	65	511	951	1.86[c]
21	962	3		×	Started from sol. 14	193	All	103	259	28	934	2137	2.29
22	576	4		×	Started from sol. 16	193	All	59	151	46	530	1071	2.02
23	576	3			Started from DHL phases ($\chi^2_{input}=2050$)	191	All			37	539	1315	2.44
24	576	3			Renormalization added to 23	191	All	59	71	37	539	1001	1.86
25	576	3	×		Started from sol. 24	191	All	59	71	69	507	990	1.95
26	576	4			Started from sol. 24	191	All	59	92	51	525	988	1.88
27	576	3			Started from DHL phases, F waves fixed	191	All			29	547	1398	2.56
28	576	3			Renormalization added to 27	191	All	59	72	29	547	1067	1.95
29	576	3			F waves varied in 28	191	All	59	74	37	539	1002	1.86
30	576	2			Started from AM solution ($\chi^2_{input}=10\,175$)	195	All	59	183	20	556	1903	3.42
31	576	2			Started from McKinley sol. ($\chi^2_{input}=4495$)	193	All	59	99	17	559	1176	2.10
32	576	3			Started from sol. 31	193	All	59	99	28	548	1153	2.10

[a] HW = Hamilton and Woolcock; s.l. = scattering length; res. = resonance; DHL = Donnachie, Hamilton, and Lea; AM = Anderson and Metropolis.
[b] See Ref. 3.
[c] We do not regard this solution as a good solution because of unreasonable behavior of the absorption parameters.

value. The above exploration proceeds by doubling each successive increment (starting with a small arbitrary value) for not more than a specified maximum number of times. If χ^2 is still decreasing, the exploration is terminated and the parameter is modified by the last increment. χ^2 is expected to depend approximately quadratically on each parameter in a sufficiently small neighborhood of the minimizing parameter value, but not for very large changes, hence the termination of the exploration procedure.

One further modification of the grid search method, while not used in obtaining the results reported here, deserves mention, and is soon to be incorporated in our calculation. From the interpolating parabola used to approximate the χ^2-minimizing value for nonlinear parameters in a given cycle, one can directly obtain a good estimate of the parameter increment which will result in a χ^2 increase of one, keeping fixed the values of the other parameters. This increment seems to be a good choice for the starting value for the exploration in the next cycle, at least near convergence when the parameters change by only small amounts from cycle to cycle. One needs an increment large enough to accurately define the parabola, but not so large that the χ^2 dependence is very different from parabolic. Also, this increment gives a crude indication of relative accuracy of definition of the parameters, in the sense that diagonal elements of the error matrix give a precise measure. Since it provides a lower bound for these diagonal elements, it accurately indicates poorly defined parameters.

This search scheme is applied to each parameter successively, in an arbitrarily specified order, until all parameters have been treated; then the cycle is started over again with the first nonlinear parameter. To attain some of the efficiency of a gradient search method, without the more complicated calculation, provision is made to exclude from search for a specified number of cycles parameters which have not contributed a significant decrease in χ^2 in previous cycles.

The χ^2-minimizing values of the parameters of the second (linear) type, viz., the normalization factors,

are obtained exactly by quadratically fitting three points for each parameter individually. (χ^2 is precisely quadratic in each.) However, since the determination of the nonlinear type of parameters is approximate, and since the χ^2-minimizing value of any linear parameter is correlated with all nonlinear parameters, the normalization factors are "searched" less frequently than each cycle, but several times before the search is terminated with parameter values to be called final.

Because of the approximations involved in this search method, χ^2 will continue to decrease by, typically, a tenth of a percent per cycle for a large number of cycles after the χ^2-minimizing solution has essentially been determined. Therefore, an arbitrary convergence criterion on χ^2 must be specified to avoid needless, indeed useless, calculation.

The determination of the arbitrary elements of this search method is a matter of experience. Examples can be constructed in which this scheme will fail to locate the true χ^2-minimizing values of the parameters, but this is not a characteristic which is unique to this scheme. In any case, this method seems to be adequate for the physical problem reported here. Comparisons of this search scheme with those used by other investigators have been carried out at Livermore in connection with nucleon-nucleon phase-shift analyses.[28] The results indicate that the method used here is at least as adequate as others. In particular, the termination of search based on a χ^2 convergence criterion yields parameter values unique to within a small fraction of the parameter errors where these have been calculated.

VI. 0–350-MeV RESULTS

Some of the 0–350-MeV calculations are summarized in Table II. It is obvious from the table that one needs only partial waves up through F waves ($l_m=3$) in the 0–350-MeV energy range. In fact, $l_m=2$ is sufficient to obtain the general character of the large phases. The 0–350-MeV data are not capable of precisely defining the small absorption near the end of the energy range. Unreasonable behavior for the absorption parameters is obtained when absorption is allowed. Agreement in the larger phases with the Yale results[6] is quite good. The small phases (F phases and some D phases) apparently have large error bands. We are presently developing a computer code to calculate errors in the phases.

As early as 1956 Anderson and Metropolis[29] (AM) did a pion-nucleon energy-dependent phase-shift analysis. They used the data then available (327 data) from 0 to 300 MeV and included only S and P waves. Their parametrization is similar to ours except that only odd powers of k are used in our Eq. (4) and their form for the P_{33} resonance is simpler. We have carried out a fit to our data selection using as input the AM solution. Following them we used only odd powers of k; however, we allowed D waves. The result is solution 30 of Table II. The initial χ^2 with no data renormalized is 10 175 and the final χ^2 is 1900.

McKinley[2] has fit single energy phase shifts with equations similar to our Eq. (4). He used only odd powers of k. Using his Eqs. (1), (4), (5), (6), and (9) and the Layson resonance form[16] for the P_{33} state as input, we get an initial χ^2 of 4495 with no data renormalized. The final χ^2 is 1176, where we have allowed D waves ($l_m=2$). When we use $l_m=3$, we get $\chi^2=1153$. The results are solutions 31 and 32 of Table II.

Recently Donnachie, Hamilton, and Lea (DHL) have predicted the P (except P_{11}), D, and F waves from 0 to 400 MeV using a peripheral model and partial-

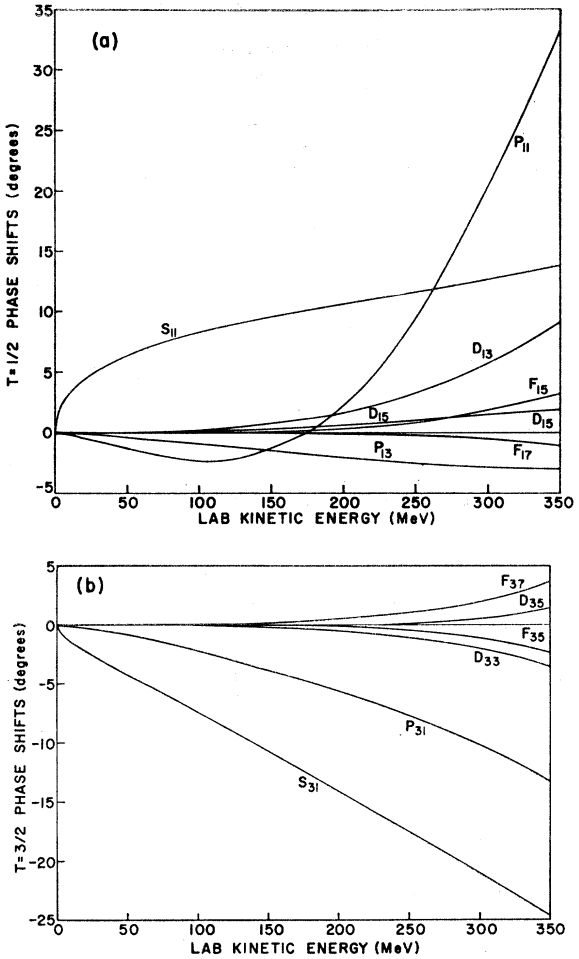

FIG. 2. Phase shifts for 0–350-MeV solution 24 of Table II. (The P_{33} phase shift is not shown. It is the same as for the 0–700-MeV solution in Fig. 3.) This solution was obtained by using Donnachie, Hamilton, and Lea's predictions for the P (except P_{11}), D, and F waves (Ref. 30) and is the best solution we have. (a) $T=\frac{1}{2}$ phase shifts. (b) $T=\frac{3}{2}$ phase shifts.

[28] R. A. Arndt, Lawrence Radiation Laboratory, Livermore, California (private communication).

[29] H. L. Anderson, *Proceedings of the Sixth Annual Rochester Conference* (Interscience Publishers, Inc., New York, 1956), p. 1–20. The coefficient c_3 should be $+0.0078$ rather than -0.0078.

TABLE III. The parameters in the energy-dependent form [Eq. (4)] for the phase shifts for the 0–350-MeV solution 24 of Table II. This solution was obtained by using Donnachie, Hamilton, and Lea's predictions for the P (except P_{11}), D, and F waves (Ref. 30) and is the best 0–350-MeV solution we have.

State	a_0	a_1	a_2	a_3	q_{0_π}
S_{11}	$+0.195530$	-0.077224	$+0.016471$	-0.2299×10^{-4}	
S_{31}	-0.062897	-0.038534	-0.008068	$+0.8734\times10^{-4}$	
P_{11}	-0.100852	$+0.064993$	$+0.3796\times10^{-4}$		
P_{31}	-0.052532	$+0.029051$	-0.006173		
P_{13}	-0.021752	$+0.010737$	-0.001356		
P_{33}	0	0	0		1.914
D_{13}	$+0.001929$	$+0.1559\times10^{-3}$			
D_{33}	-0.1609×10^{-3}	-0.3038×10^{-3}			
D_{15}	$+0.001745$	-0.5365×10^{-3}			
D_{35}	-0.001185	$+0.6529\times10^{-3}$			
F_{15}	$+0.2516\times10^{-3}$	-0.4437×10^{-4}			
F_{35}	-0.6241×10^{-4}	-0.1785×10^{-4}			
F_{17}	-0.1814×10^{-4}	-0.1229×10^{-4}			
F_{37}	$+0.2648\times10^{-3}$	-0.4306×10^{-4}			

TABLE IV. The values of the phase shifts in degrees at several energies for the 0–350-MeV solution 24 of Table II.

E_π (MeV)	S_{11}	S_{31}	P_{11}	P_{31}	P_{13}	P_{33}	D_{13}	D_{33}	D_{15}	D_{35}	F_{15}	F_{35}	F_{17}	F_{37}
6	2.599	−1.078	−0.082	−0.044	−0.018	0.231	0.000	−0.000	0.000	−0.000	0.000	−0.000	−0.000	0.000
20	4.414	−2.257	−0.429	−0.246	−0.104	1.446	0.003	−0.000	0.002	−0.001	0.000	−0.000	−0.000	0.000
31	5.295	−3.031	−0.755	−0.455	−0.193	2.862	0.009	−0.001	0.006	−0.003	0.000	−0.000	−0.000	0.000
58	6.780	−4.795	−1.549	−1.083	−0.457	7.952	0.048	−0.010	0.030	−0.015	0.003	−0.001	−0.000	0.004
98	8.235	−7.345	−2.249	−2.203	−0.909	20.954	0.207	−0.049	0.113	−0.045	0.025	−0.010	−0.004	0.026
120	8.855	−8.766	−2.189	−2.887	−1.167	32.360	0.370	−0.094	0.187	−0.064	0.053	−0.023	−0.009	0.057
140	9.356	−10.077	−1.762	−3.544	−1.400	46.310	0.580	−0.156	0.274	−0.080	0.096	−0.044	−0.018	0.104
170	10.036	−12.079	−0.318	−4.589	−1.736	72.383	1.028	−0.296	0.439	−0.089	0.203	−0.099	−0.041	0.220
194	10.542	−13.709	1.643	−5.481	−1.985	92.650	1.525	−0.462	0.600	−0.076	0.338	−0.174	−0.073	0.368
200	10.665	−14.120	2.257	−5.713	−2.044	97.059	1.671	−0.512	0.644	−0.068	0.381	−0.199	−0.083	0.414
220	11.070	−15.500	4.680	−6.514	−2.231	109.472	2.226	−0.707	0.800	−0.026	0.550	−0.299	−0.127	0.599
240	11.471	−16.892	7.703	−7.362	−2.400	118.748	2.895	−0.951	0.969	0.046	0.769	−0.437	−0.187	0.840
270	12.073	−18.996	13.365	−8.738	−2.617	128.477	4.140	−1.424	1.239	0.228	1.209	−0.729	−0.318	1.327
290	12.480	−20.406	17.832	−9.737	−2.736	133.116	5.146	−1.821	1.426	0.412	1.588	−0.998	−0.439	1.749
310	12.896	−21.817	22.746	−10.811	−2.835	136.780	6.306	−2.293	1.612	0.657	2.048	−1.337	−0.593	2.261
333	13.388	−23.439	28.765	−12.149	−2.923	140.143	7.840	−2.937	1.820	1.027	2.685	−1.833	−0.820	2.974
345	13.652	−24.283	31.978	−12.894	−2.958	141.624	8.730	−3.321	1.923	1.264	3.069	−2.143	−0.963	3.405

TABLE V. Comparison of solutions 24, 28, and 29 of Table II at 345 MeV.

	Solution 24 of Table II (F waves varied)	Solution 28 of Table II (F waves fixed)	Solution 29 of Table II (Sol. 28 with F waves varied)		Solution 24 of Table II (F waves varied)	Solution 28 of Table II (F waves fixed)	Solution 29 of Table II (Sol. 28 with F waves varied)
S_{11}	13.65	16.08	15.22	D_{15}	1.92	1.84	1.96
S_{31}	−24.28	−24.63	−23.84	D_{35}	1.26	0.33	0.28
P_{11}	31.98	31.29	31.72	F_{15}	3.07	1.06	2.51
P_{31}	−12.89	−11.51	−11.82	F_{35}	−2.14	−0.19	−1.55
P_{13}	−2.96	−2.89	−2.85	F_{17}	−0.96	−0.19	−0.95
P_{33}	141.62	141.62	141.62	F_{37}	3.41	0.72	2.62
D_{13}	8.73	7.09	7.94	χ^2	1001	1067	1002
D_{33}	−3.32	−1.49	−2.31				

wave dispersion relations.[30] Solutions 23 through 26 in Table II were obtained by starting with their prediction and the S_{11}, S_{31}, and P_{11} phases of solution 16. The input χ^2 with no data renormalized is 2050 and the final χ^2 is 1000. Note that there is less renormalization for this solution than for the other solutions. This is the best solution we have obtained, although the final phases differ considerably from the input phases. The final F phases are considerably larger in magnitude than the DHL phases. Also, the D_{35} becomes positive at approximately 225 MeV contrary to the DHL prediction. The reduced elastic width γ^2 of the P_{33} resonance was allowed to vary from the value of 0.133 obtained by Layson, but did not do so. Solution 24 is shown in Fig. 2. Lists of the final parameters are given in Table III and the values of the phase shifts at several energies are given in Table IV. When we fixed the F waves at the DHL values we obtained solution 28 of Table II with a χ^2 of 1067. Then upon allowing the F waves to vary, χ^2 went down to 1000 again (solution 29). However, solution 29 is closer to solution 28 than

[30] A. Donnachie, J. Hamilton, and A. T. Lea, Phys. Rev. **135**, B515 (1964).

TABLE VI. The characteristics of some of the 0–700-MeV calculations. $\bar{\gamma}^2$ is related to γ^2 by $\gamma^2=0.133\bar{\gamma}^2$.

Solution	No. of data	l_m	Special features	E_{π_r} (P_{33}) (MeV)	E_{π_r} (MeV)	$\bar{\gamma}^2$ (P_{33})	$\bar{\gamma}^2$	$\bar{\Gamma}_{in}$ (P_{33})	$\bar{\Gamma}_{in}$	Tanδ param.	No. of norm parameters	χ^2_{norm}	No. of parameters	Expected χ^2	χ^2	χ^2/χ^2_{exp}
1	835	3	D_{13} res. at 600 MeV. Started from σ_T fit	193	670				0.0112	All	68	215	67	768	2131	2.77
2	835	3	P_{13} res. at 600 MeV. Started from σ_T fit	196	751 (limit)				0.0494	All	68	384	67	768	3803	4.95
3	835	3	No res. Started from σ_T fit	193						All	68	314	65	770	2668	3.46
4	835	3	D_{13} and P_{13} res. at 600 MeV. Started from σ_T fit	Puts in such a large $\bar{\Gamma}_{in}$ for the D_{13} res. that it causes the phase shift to go through 0°[a]						All	68	432	69	766	3569	4.66
5	835	3	P_{11} res. at 600 MeV. Started from σ_T fit	192	615				0.0255	All	68	306	67	768	3487	4.54
6	835	3	Started from 1	193	668				0.0124	None	68	223	67	768	2074	2.70
7	835	3	Started from 3	193						All but P_{11}, P_{13}, and D_{13}	68	316	65	768	2629	3.42
8	1171	3	Started from 6	193	676				0.0116	None	85	350	67	1104	3490	3.16
9	1171	3	Started from 8	192	662	0.9862	0.8630	0.0274	0.0116	None	85	325	70	1101	3370	3.06
10	1171	4	Started from 8	193	638	1.00	0.6522	0.0	0.0123	None	85	217	106	1065	2810	2.64
11	1173	4	Started from 10 [$\sigma(0)$ errors reduced]	193	638	1.00	0.6442	0.0	0.0123	None	85	220	106	1067	2862	2.68
12	1173	5	Started from 11	193	638	1.00	0.6378	0.0	0.0125	None	85	226	150	1023	2825	2.76
13	1173	3	Started from 7	193						All but P_{11}, P_{13}, and D_{13}	85	449	65	1108	4556	4.11
14	1173	4	Started from 11 except "modified" Layson form used for P_{11}	193	638-D_{13} 585-P_{11}[b]	1.00	0.6561-D_{13} 3.682-P_{11}	0.0	0.0121-D_{13} 0.3885-P_{11}	None	85	218	110	1063	2777	2.61
15	1173	4	Started from 11 except $P_{11}<90°$	193	639	1.00	0.6088	0.0	0.0116	P_{11} only	85	221	106	1067	2861	2.68
16	1173	4	Started from 11 except $P_{11}<45°$	193	655	1.00	0.6631	0.0	0.0172	None	85	225	102	1071	3031	2.83
17	1173	4	P_{11} allowed to vary in solution 16	193	639	1.00	0.5876	0.0	0.0133	None	85	221	106	1067	2762	2.59

[a] See M. B. Watson, M. Ferro-Luzzi, and R. D. Tripp, Phys. Rev. 131, 2248 (1963).
[b] The P_{11} phase shift passes through zero degrees at 150 MeV.

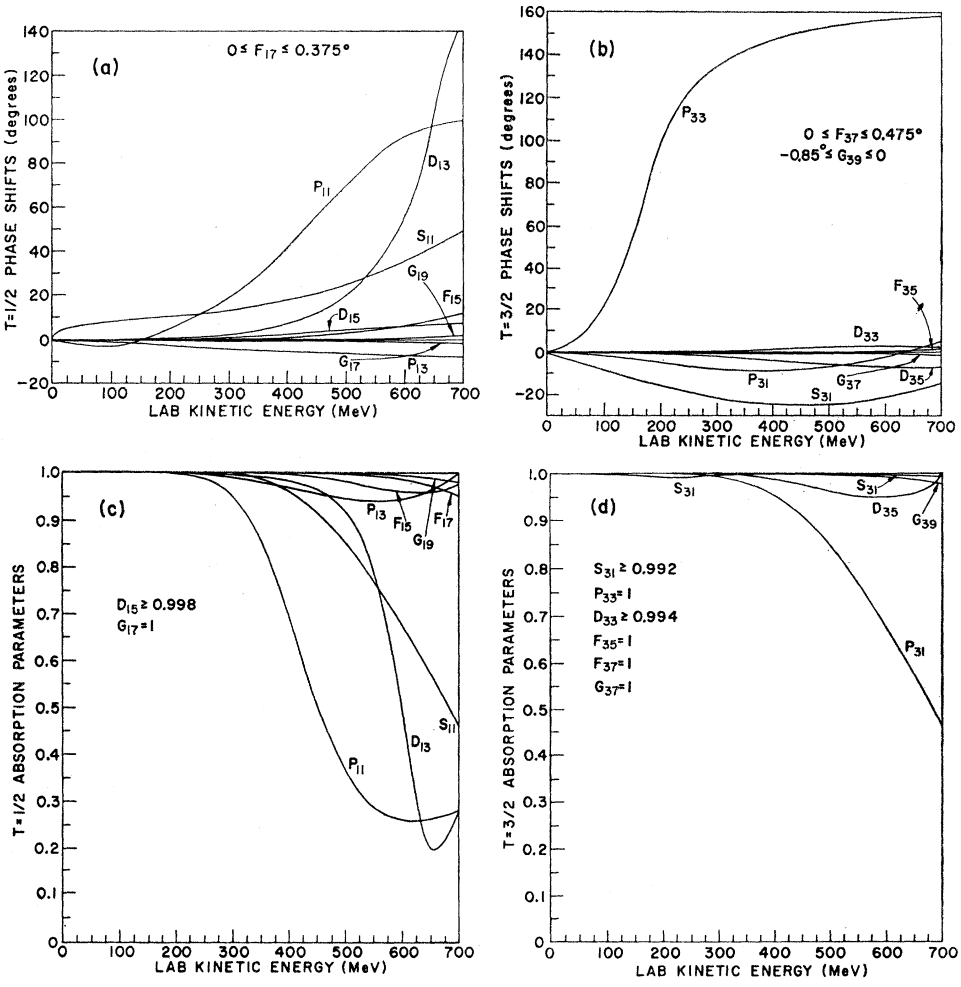

FIG. 3. Phase shifts and absorption parameters for 0–700-MeV solution 14 of Table V. (a) $T=\frac{1}{2}$ phase shifts. (b) $T=\frac{3}{2}$ phase shifts. (c) $T=\frac{1}{2}$ absorption parameters. (d) $T=\frac{3}{2}$ absorption parameters.

is solution 24. One can see this from Table V, which lists the phases at 345 MeV for the three solutions.

The large ratios of χ^2 to the "expected" χ^2 are undoubtedly due to two main causes: (1) the inconsistencies among the data, and (2) the fact that the energy-dependent forms can at best only approximate the actual shape.

VII. 0–700- AND 300–800-MeV RESULTS

We have attempted to fit the 0–700-MeV data with several assumptions about the prominent states at about 600 MeV. The results are given in Table VI. A D_{13} resonance gives a significantly better fit than a P_{13} resonance or than when no resonance at all is built in.[31] (We also tried D_{13} and P_{13} resonances together, but the data violently exclude this possibility.) In all three of these cases the P_{11} resonance occurs automatically when Eq. (5) is used for it. In the no-resonance case, the D_{13} phase goes only to about 25° at 700 MeV.

[31] B. T. Feld and L. D. Roper, *Proceedings of the Sienna International Conference on Elementary Particles* (Italian Physical Society, Bologna, 1963), p. 400.

Changing from $l_m=3$ to $l_m=4$ significantly decreases χ^2 for the D_{13} resonance fit; however, changing to $l_m=5$ changes χ^2 very little. The main difference between the $l_m=3$ fit and the $l_m=4$ fit is in fitting the high-energy polarization data. (Comparison of the D_{13} solution's predictions for observables to the experimental observables have been given elsewhere.[26])

Attempts have been made to keep the P_{11} phase shift less than 25°, but we were never able to obtain decent χ^2's with this restriction. After keeping it less than 25° until a minimum χ^2 (about 7000) was found, it went back to resonance immediately when allowed to do so. Allowing the elastic reduced width of the D_{13} resonance to vary[3] before allowing the P_{11} to resonate did not change the situation. However, we obtained good fits when we used Eq. (4) for the P_{11} phase shift, which restricts it to be less than 90°. Even in this case, it is large (about 80°) at 700 MeV. We also tried to achieve a fit by keeping the P_{11} phase fixed at less than 45°. Solution 16 of Table VI is the result. The χ^2 is not much higher than for the case of the P_{11} resonance, thus showing the relative insensitivity of the data to

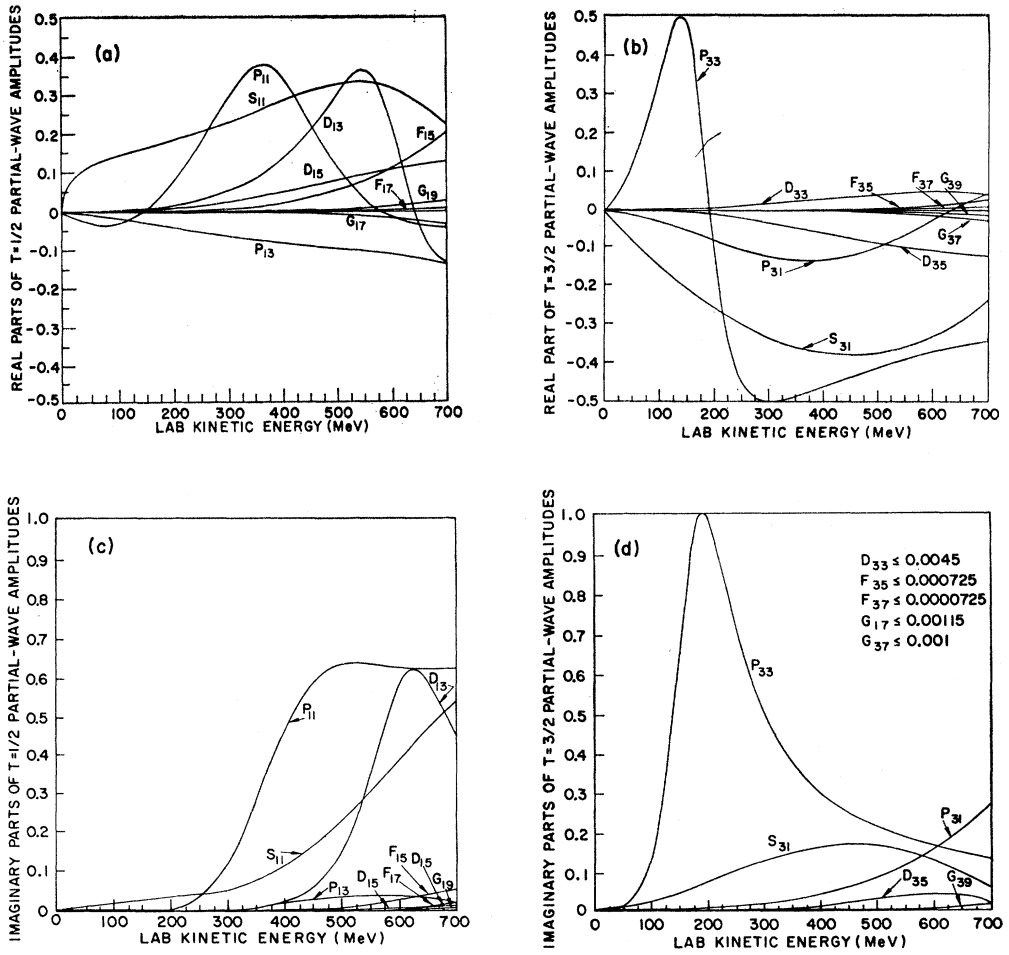

FIG. 4. Real and imaginary parts of the partial-wave amplitudes for 0–700-MeV solution 14 of Table V. (a) Real parts of $T=\frac{1}{2}$ partial-wave amplitudes. (b) Real parts of $T=\frac{3}{2}$ partial-wave amplitudes. (c) Imaginary parts of $T=\frac{1}{2}$ partial-wave amplitudes. (d) Imaginary parts of $T=\frac{3}{2}$ partial-wave amplitudes.

large variations in the P_{11} phase shift. When we freed the P_{11} phase shift, it became large and went through 90° at 610 MeV (solution 17 of Table VI).

Since the P_{11} phase shift is negative at low energies, the Layson resonance form[16] will not work for it. We have found that putting in the Layson form for the P_{11} does not yield good fits. However, we obtain the best fit of all by using a "modified" Layson form for the P_{11} in which we replace Γ_{el} by $\Gamma_{el}(q_0-q_{0_z})/q_0$, where q_{0_z} is the position where the phase shift changes sign in terms of the pion c.m. total energy. This is solution 14 of Table VI. The ratio of χ^2 to the expected χ^2 is 2.61.

We did a 300–800-MeV analysis for the purpose of trying to represent the P_{11} state by the unmodified Layson resonance form. Comparable fits were obtained both with the Layson form and with the parametrization of Eq. (5), although the latter is slightly better. However, the position of the P_{11} resonance was considerably different for the two fits; the latter giving the position at 585 MeV and the Layson-form resonance being at 747 MeV, well above the D_{13} resonance. This again shows the relative insensitivity of the data to

TABLE VII. The characteristics of the 300–800-MeV calculations. In each case 954 data were used and there are 51 normalization parameters. $l_m=4$ in each case.

Solution	$E_{\pi r}$ (P_{33}) (MeV)	$E_{\pi r}$ (MeV)	$\bar{\gamma}^2$ (P_{33})	$\bar{\gamma}^2$	$\bar{\Gamma}_{in}$ (P_{33})	$\bar{\Gamma}_{in}$	Tanδ param.	χ^2_{norm}	No. of parameters	Expected χ^2	χ^2	χ^2/χ^2_{exp}
1[a]	199	638	0.9559	0.6183	0.0	0.0114	None	150	106	848	2706	3.19
2[b]	192	{747-P_{11} 636-D_{13}}	0.9841	{2.1102-P_{11} 0.6154-D_{13}}	0.008	{0.5238-P_{11} 0.0115-D_{13}}	None	176	109	845	2780	3.29
3[c]	200	640	0.9415	0.6048	0.0	0.0110	P_{11} only	170	106	848	2810	3.31

[a] Started from solution 11 of Table VI.
[b] Started from solution 11 of Table VI except res. form for P_{11}.
[c] Started from solution 1 except $P_{11}<90°$.

TABLE VIII. The parameters in the energy-dependent form for the phase shifts [Eq. (5)] and for the absorption parameters for the 0–700-MeV solution 14 of Table VI.

State	a_0	a_1	a_2	a_3	a_4	q_{0r}	$\bar{\gamma}^2$	q_{0z}
				Phase-shift coefficients				
S_{11}	+0.212352	−0.104657	+0.032823	−0.006891	+0.001916			
S_{31}	−0.024330	−0.108591	+0.006051	+0.005377	$+0.1594\times10^{-3}$			
P_{11}	-0.2181×10^{-7}	-0.6449×10^{-7}	-0.1861×10^{-9}	$+0.1272\times10^{-8}$	a	3.337	3.682	1.736
P_{31}	−0.032514	+0.007879	$+0.6727\times10^{-3}$	-0.3267×10^{-4}				
P_{13}	−0.017520	+0.006601	-0.5203×10^{-3}	-0.5623×10^{-4}				
P_{33}	$+0.8965\times10^{-10}$	$+0.1187\times10^{-8}$	$+0.6440\times10^{-9}$	$+0.1849\times10^{-9}$	a	1.923	1.00	
D_{13}	−0.001019	$+0.3439\times10^{-3}$	-0.9397×10^{-5}		a	3.494	0.6561	
D_{33}	$+0.7760\times10^{-3}$	-0.1710×10^{-3}	-0.7837×10^{-5}					
D_{15}	$+0.8688\times10^{-3}$	-0.1049×10^{-3}	-0.2115×10^{-4}					
D_{35}	−0.001554	$+0.3913\times10^{-3}$	-0.4670×10^{-5}					
F_{15}	$+0.3498\times10^{-4}$	-0.1116×10^{-5}						
F_{35}	$+0.2105\times10^{-5}$	$+0.4920\times10^{-6}$						
F_{17}	$+0.1107\times10^{-4}$	-0.2895×10^{-5}						
F_{37}	$+0.8397\times10^{-6}$	$+0.1073\times10^{-6}$						
G_{17}	-0.3891×10^{-6}							
G_{37}	-0.3361×10^{-6}							
G_{19}	$+0.3330\times10^{-6}$							
G_{39}	-0.1706×10^{-6}							
	b_0	b_1	b_2	b_3	b_4			Γ_{in}
				Absorption parameter coefficients				
S_{11}	+0.010377	−0.040059	+0.032726	+0.011179	+0.001392			
S_{31}	+0.029141	−0.069753	+0.054314	−0.013257	-0.4173×10^{-5}			
P_{11}	+0.038733	−0.003904	−0.002724	+0.002320	a			0.3885
P_{31}	−0.002736	+0.022741	−0.001462	$+0.7920\times10^{-3}$				
P_{13}	+0.019510	−0.004176	-0.4831×10^{-4}	−0.001229				
P_{33}	0	0	0	0				0
D_{13}	$+0.7258\times10^{-3}$	-0.3519×10^{-3}	-0.3827×10^{-6}		a			0.01211
D_{33}	-0.1474×10^{-4}	$+0.2730\times10^{-5}$	$+0.2038\times10^{-4}$					
D_{15}	$+0.2138\times10^{-3}$	-0.2247×10^{-6}	-0.5031×10^{-4}					
D_{35}	+0.007394	−0.001345	−0.001086					
F_{15}	+0.002372	−0.001119						
F_{35}	0	0						
F_{17}	-0.7193×10^{-4}	$+0.1152\times10^{-3}$						
F_{37}	0	0						
G_{17}	0							
G_{37}	0							
G_{19}	$+0.1516\times10^{-4}$							
G_{39}	$+0.1740\times10^{-4}$							

[a] Background to the resonance. See Sec. III.

large variations in the phase shift. The results are shown in Table VII.

Solution 14 of Table VI is shown in Figs. 3 and 4. Lists of the final parameters and the values of the phase shifts and the absorption parameters are given in Tables VIII and IX, respectively.

VIII. 0–100- AND 0–50-MeV RESULTS

To check for consistency with the 0–350-MeV analysis we did a 0–100-MeV analysis using all available data (197 data). Writing the S and P phases according to

$$\tan\delta = ak^{2l+1},$$

except for a resonance in the P_{33} state and searching from various input, we get the results shown in Table X. The fact that such different input as used in parts A and D of Table X yield the same solution lead us to believe that we have a unique solution, even though the χ^2's are high. The high χ^2's are largely due to the fact that we have not discarded any data, some of which are highly inconsistent with each other.

The fit is improved by using higher powers of k in the parametrization. Table XI gives some solution characteristics when four coefficients are used.

Our main object in doing this low-energy analysis was to establish whether or not the P_{11} is negative below about 150 MeV. We feel that this is definitely established.

The 0–50-MeV analysis (92 data) yielded several possible solutions with different P_{11}, P_{13}, and P_{31} phases; however, the S_{11}, S_{31}, and P_{33} phases agree very well with the higher energy solutions. The P_{13} and P_{31} phases are always negative but vary widely in magnitude. The P_{11} phase varies between slightly positive and the values found in the 0–100-MeV analysis.

The 0–100-MeV (solution B of Table XI), 0–350-MeV (solution 24 of Table II), and 0–700-MeV (solution 11 of Table VI) phases are compared in Fig. 5. Also plotted are several single energy phase shifts.

TABLE IX. The values of the phase shifts and absorption parameters at several energies for the 0–700-MeV solution 14 of Table VI.

E_π (MeV)	S_{11}	S_{31}	P_{11}	P_{31}	P_{13}	P_{33}	D_{13}	D_{33}	D_{15}	D_{35}	F_{15}	F_{35}	F_{17}	F_{37}	G_{17}	G_{37}	G_{19}	G_{39}
								Phase shifts										
6	+2.758	−0.761	−0.150	−0.030	−0.015	+0.228	0	0	0	0	0	0	0	0	0	0	0	0
31	+5.483	−2.934	−1.220	−0.336	−0.168	+2.818	+0.005	+0.003	+0.003	−0.006	0	0	0	0	0	0	0	0
58	+6.920	−5.135	−2.045	−0.847	−0.412	+7.810	+0.029	+0.015	+0.018	−0.028	+0.001	0	0	0	0	0	0	0
98	+8.293	−8.305	−2.060	−1.818	−0.863	+20.475	+0.122	+0.057	+0.071	−0.110	+0.004	0	+0.001	0	0	0	0	0
120	+8.880	−9.996	−1.458	−2.422	−1.139	+31.526	+0.214	+0.096	+0.123	−0.187	+0.009	+0.001	+0.002	0	0	0	0	0
144	+9.458	−11.785	−0.344	−3.113	−1.454	+48.152	+0.357	+0.154	+0.200	−0.300	+0.019	+0.002	+0.004	+0.001	0	0	0	0
170	+10.055	−13.642	+1.375	−3.879	−1.805	+70.594	+0.659	+0.236	+0.313	−0.459	+0.037	+0.003	+0.007	+0.001	−0.001	−0.001	+0.001	0
195	+10.632	−15.334	+3.522	−4.610	−2.146	+91.699	+0.840	+0.334	+0.452	−0.651	+0.064	+0.006	+0.012	+0.002	−0.002	−0.002	+0.002	−0.001
220	+11.237	−16.920	+6.166	−5.317	−2.486	+108.122	+1.186	+0.452	+0.622	−0.882	+0.105	+0.009	+0.019	+0.003	−0.004	−0.003	+0.003	−0.002
240	+11.756	−18.104	+8.659	−5.853	−2.755	+117.680	+1.527	+0.560	+0.782	−1.095	+0.150	+0.014	+0.026	+0.005	−0.006	−0.005	+0.005	−0.003
270	+12.616	−19.723	+13.090	−6.586	−3.151	+127.720	+2.161	+0.744	+1.062	−1.459	+0.243	+0.023	+0.039	+0.008	−0.012	−0.010	+0.010	−0.005
310	+13.959	−21.563	+20.416	−7.389	−3.658	+136.274	+3.297	+1.025	+1.509	−2.023	+0.430	+0.042	+0.063	+0.014	−0.024	−0.021	+0.021	−0.011
333	+14.857	−22.442	+25.391	−7.738	−3.938	+139.728	+4.142	+1.201	+1.803	−2.383	+0.578	+0.057	+0.080	+0.019	−0.036	−0.031	+0.031	−0.016
370	+16.526	−23.559	+34.422	−8.093	−4.371	+143.947	+5.895	+1.500	+2.328	−3.006	+0.894	+0.091	+0.113	+0.030	−0.063	−0.054	+0.054	−0.028
410	+18.689	−24.331	+45.116	−8.146	−4.814	+147.312	+8.549	+1.832	+2.957	−3.723	+1.367	+0.143	+0.154	+0.047	−0.109	−0.095	+0.094	−0.048
450	+21.278	−24.622	+56.131	−7.805	−5.237	+149.890	+12.403	+2.155	+3.636	−4.460	+2.008	+0.216	+0.201	+0.071	−0.181	−0.156	+0.155	−0.079
490	+24.345	−24.406	+67.115	−7.024	−5.647	+151.944	+18.185	+2.445	+4.342	−5.184	+2.853	+0.315	+0.251	+0.103	−0.286	−0.247	+0.244	−0.125
523	+27.271	−23.831	+75.906	−6.017	−5.982	+153.356	+25.282	+2.643	+4.930	−5.742	+3.732	+0.421	+0.290	+0.137	−0.406	−0.350	+0.347	−0.178
550	+29.951	−23.084	+82.545	−4.933	−6.259	+154.366	+33.420	+2.764	+5.403	−6.168	+4.591	+0.526	+0.320	+0.170	−0.531	−0.459	+0.455	−0.233
572	+32.336	−22.287	+87.298	−3.867	−6.489	+155.110	+42.079	+2.830	+5.775	−6.476	+5.393	+0.625	+0.341	+0.201	−0.656	−0.567	+0.561	−0.288
581	+33.366	−21.911	+89.028	−3.382	−6.585	+155.396	+46.233	+2.847	+5.922	−6.591	+5.750	+0.670	+0.349	+0.216	−0.713	−0.616	+0.610	−0.313
600	+35.647	−21.023	+92.228	−2.263	−6.792	+155.970	+56.396	+2.861	+6.223	−6.809	+6.561	+0.772	+0.362	+0.248	−0.847	−0.732	+0.725	−0.372
616	+37.683	−20.174	+94.437	−1.218	−6.971	+156.423	+66.965	+2.849	+6.461	−6.965	+7.307	+0.867	+0.369	+0.278	−0.976	−0.843	+0.835	−0.428
650	+42.373	−18.057	+97.737	+1.323	−7.374	+157.308	+101.331	+2.738	+6.914	−7.195	+9.103	+1.100	+0.372	+0.351	−1.300	−1.123	+1.113	−0.570
689	+48.391	−15.094	+99.602	+4.797	−7.881	+158.212	+138.934	+2.444	+7.316	−7.258	+11.544	+1.423	+0.345	+0.450	−1.775	−1.533	+1.519	−0.778
698	+49.881	−14.328	+99.809	+5.687	−8.007	+158.405	+143.921	+2.348	+7.387	−7.238	+12.171	+1.507	+0.334	+0.478	−1.902	−1.643	+1.627	−0.834
								Absorption parameters										
170	0.999	0.998	1.000	1.000	1.000	1.000	1.000	1.000	1.000	1.000	1.000	1.000	1.000	1.000	1.000	1.000	1.000	1.000
195	0.998	0.994	1.000	1.000	1.000	1.000	1.000	1.000	1.000	1.000	1.000	1.000	1.000	1.000	1.000	1.000	1.000	1.000
220	0.999	0.992	0.997	1.000	0.999	1.000	0.999	1.000	1.000	1.000	1.000	1.000	1.000	1.000	1.000	1.000	1.000	1.000
240	1.000	0.993	0.993	0.999	0.998	1.000	0.999	1.000	1.000	1.000	1.000	1.000	1.000	1.000	1.000	1.000	1.000	1.000
270	1.000	0.994	0.980	0.997	0.995	1.000	0.998	1.000	1.000	0.999	1.000	1.000	1.000	1.000	1.000	1.000	1.000	1.000
310	0.997	0.997	0.938	0.991	0.989	1.000	0.995	1.000	1.000	0.998	1.000	1.000	1.000	1.000	1.000	1.000	1.000	1.000
333	0.992	0.998	0.897	0.985	0.985	1.000	0.993	1.000	1.000	0.996	0.999	1.000	1.000	1.000	1.000	1.000	1.000	1.000
370	0.987	0.999	0.796	0.971	0.976	1.000	0.989	1.000	1.000	0.992	0.998	1.000	1.000	1.000	1.000	1.000	1.000	1.000
410	0.953	0.999	0.651	0.946	0.966	1.000	0.980	1.000	1.000	0.986	0.996	1.000	1.000	1.000	1.000	1.000	1.000	1.000
450	0.916	0.998	0.502	0.910	0.956	1.000	0.964	1.000	0.999	0.977	0.991	1.000	1.000	1.000	1.000	1.000	1.000	1.000
490	0.866	0.996	0.383	0.863	0.947	1.000	0.932	1.000	0.999	0.966	0.984	1.000	0.998	1.000	1.000	1.000	0.999	0.999
523	0.816	0.994	0.317	0.815	0.941	1.000	0.875	0.999	0.998	0.957	0.977	1.000	0.997	1.000	1.000	1.000	0.999	0.999
550	0.770	0.993	0.283	0.770	0.939	1.000	0.787	0.999	0.998	0.951	0.970	1.000	0.994	1.000	1.000	1.000	0.998	0.998
572	0.729	0.992	0.267	0.730	0.939	1.000	0.674	0.999	0.998	0.947	0.965	1.000	0.992	1.000	1.000	1.000	0.997	0.997
581	0.711	0.992	0.263	0.713	0.940	1.000	0.616	0.999	0.998	0.946	0.963	1.000	0.991	1.000	1.000	1.000	0.997	0.996
600	0.673	0.992	0.258	0.675	0.943	1.000	0.480	0.998	0.998	0.945	0.959	1.000	0.987	1.000	1.000	1.000	0.995	0.995
616	0.640	0.992	0.256	0.642	0.947	1.000	0.362	0.998	0.998	0.946	0.957	1.000	0.984	1.000	1.000	1.000	0.994	0.993
650	0.567	0.994	0.260	0.569	0.961	1.000	0.200	0.997	0.998	0.956	0.957	1.000	0.973	1.000	1.000	1.000	0.990	0.989
689	0.483	0.998	0.273	0.482	0.989	1.000	0.251	0.995	1.000	0.985	0.971	1.000	0.956	1.000	1.000	1.000	0.983	0.980
698	0.464	1.000	0.277	0.463	0.998	1.000	0.274	0.994	1.000	0.995	0.977	1.000	0.951	1.000	1.000	1.000	0.981	0.978

TABLE X. 0–100-MeV solutions for the parametrization $\tan\delta_l = ak^{2l+1}$. The pion c.m. total energy at which the P_{33} resonance occurs is q_{0r}.

Phase	Input	Output (no renormalization)	Output (renormalization)
	A. Started from Hamilton and Woolcock (HW) scattering lengths except Layson resonance form for P_{33}		
S_{11}	$a=+0.171$ ($\chi^2=3180$)	$a=+0.157$ ($\chi^2=1188$)	$a=+0.158$ ($\chi^2=1007$)
S_{31}	-0.088	-0.096	-0.097
P_{11}	-0.101	-0.039	-0.042
P_{31}	-0.038	-0.034	-0.033
P_{13}	-0.029	-0.030	-0.028
P_{33}	$q_{0r}=1.925$	$q_{0r}=1.909$	$q_{0r}=1.909$
	B. Started from HW except P_{11} started as zero		
S_{11}	$a=+0.171$ ($\chi^2=1700$)	$a=+0.157$ ($\chi^2=1188$)	
S_{31}	-0.088	-0.095	
P_{11}	0	-0.038	
P_{31}	-0.038	-0.034	
P_{13}	-0.029	-0.029	
P_{33}	$q_{0r}=1.925$	$q_{0r}=1.909$	
	C. Started from HW except P_{11} input with $a=+0.101$		
S_{11}	$a=+0.171$ ($\chi^2=3541$)	$a=+0.157$ ($\chi^2=1188$)	
S_{31}	-0.088	-0.096	
P_{11}	$+0.101$	-0.038	
P_{31}	-0.038	-0.034	
P_{13}	-0.029	-0.029	
P_{33}	$q_{0r}=1.925$	$q_{0r}=1.909$	
	D. Started from $a=0$		
S_{11}	$a=+0$ ($\chi^2=9597$)	$a=+0.157$ ($\chi^2=1188$)	
S_{31}	$+0$	-0.096	
P_{11}	$+0$	-0.038	
P_{31}	$+0$	-0.034	
P_{13}	$+0$	-0.029	
P_{33}	$q_{0r}=1.925$	$q_{0r}=1.909$	
	E. Started from solution A except P_{11} fixed with $a=0$		
S_{11}	$a=+0.157$ ($\chi^2=1490$)	$a=+0.152$ ($\chi^2=1390$)	
S_{31}	-0.096	-0.097	
P_{11}	$+0$	$+0$	
P_{31}	-0.034	-0.038	
P_{13}	-0.030	-0.015	
P_{33}	$q_{0r}=1.909$	$q_{0r}=1.908$	
	F. Started from solution A except P_{11} fixed with $a=+0.05$		
S_{11}	$a=+0.157$ ($\chi^2=2298$)	$a=+0.150$ ($\chi^2=2219$)	
S_{31}	-0.096	-0.094	
P_{11}	$+0.05$	$+0.05$	
P_{31}	-0.034	-0.040	
P_{13}	-0.030	-0.014	
P_{33}	$q_{0r}=1.909$	$q_{0r}=1.908$	

IX. DISCUSSION

The idea of parametrizing the phase shifts as functions of energy appears to be basically sound.[32] The specific parametrization we used can represent many kinds of phase-shift behavior. Other parametrizations should be used to test for dependence on the form of the parametrization. Our 0–350-MeV solution agrees in the large phases with the Yale solution[6] which uses an entirely different parametrization.

Some arguments that could be advanced against the parametrization used in this work are:

(1) The threshold behavior may not be correct. The k^{2l+1} behavior for phase shifts derived from ordinary quantum mechanics is not incontrovertible. In fact, if one assumes that the ratio of the slope to the value of the radial wave function at the interaction radius differs from that obtained in the absence of a scattering potential by a term linear in k, the momentum, the low-energy behavior is k^{2l+2}.[33] The $(k-k_0)^{2l+1}$ threshold

[32] One of the authors (L.D.R.) wishes to thank Dr. Pierre Noyes and Dr. Michael Moravcsik for stressing the importance of energy parametrization during the early planning of this analysis.

[33] W. Bryan DeFacio called our attention to this fact. See p. 107 of Schiff's book (Ref. 13).

TABLE XI. Some of the characteristics of the 0–100-MeV solutions for the parametrization $\tan\delta_l = k^{2l+1}(a_0 + a_1k + a_2k^2 + a_3k^3)$.

Solution	χ^2 (start)	χ^2 (no renormalization)	χ^2 (renormalization)	P_{11} behavior
A[a]	1440	648		P_{11} neg. to $-2.008°$ at 100 MeV
B[b]	1440	637	501	P_{11} neg. to $-2.097°$ at 100 MeV
C[c]	1700	639		P_{11} neg. to $-2.265°$ at 100 MeV
D[d]	9597	658		P_{11} neg. to $-2.192°$ at 100 MeV

[a] Started from HW plus $P_{11}a_1 = +0.065$ and scattering lengths (a_0) kept fixed.
[b] Started from HW plus $P_{11}a_1 = +0.065$.
[c] Started from HW except $P_{11}a_0 = 0$.
[d] Started from all a's at zero.

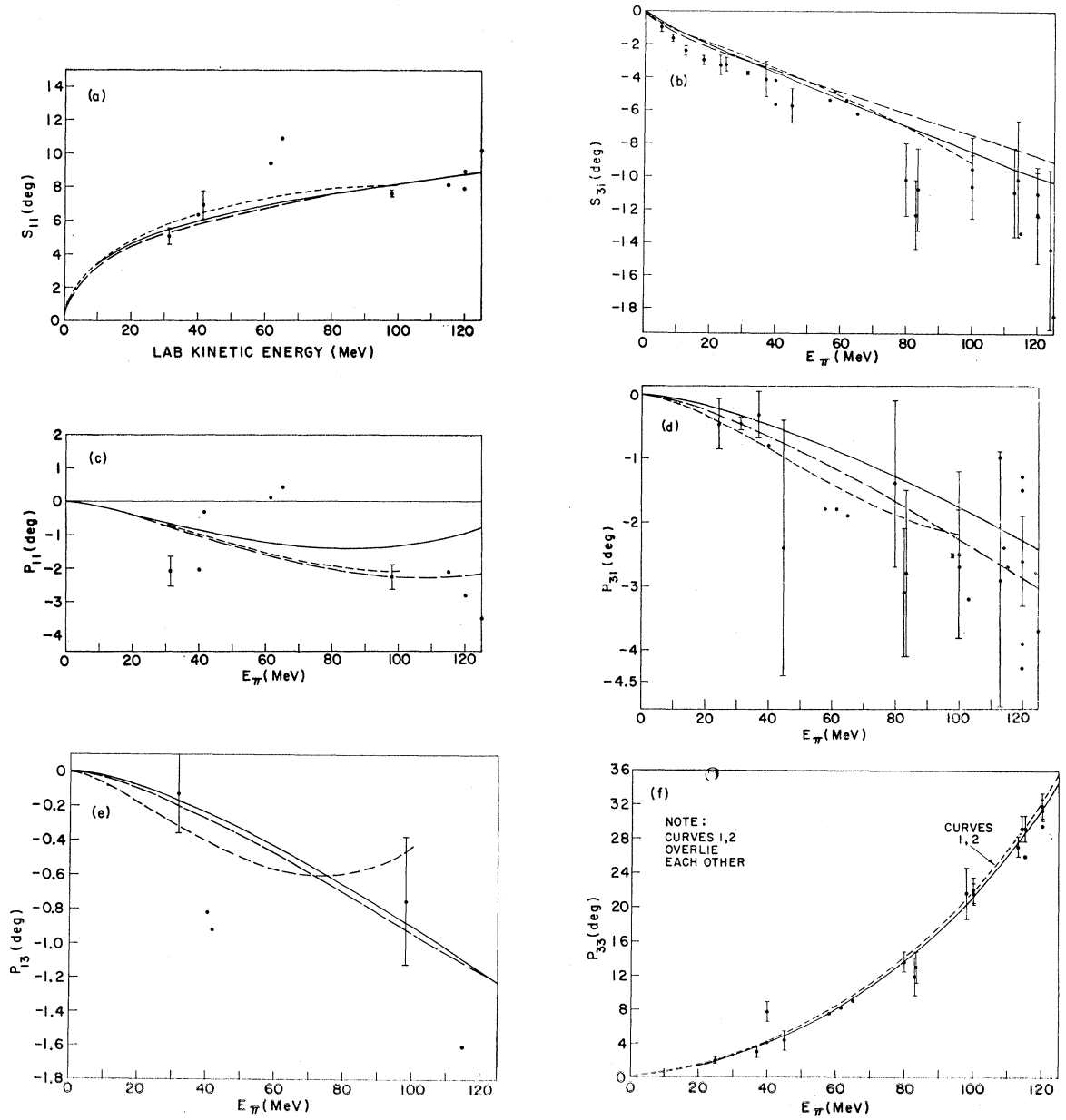

FIG. 5. Comparison of the 0–100-MeV (short dash), 0–350-MeV (long dash), and 0–700-MeV (solid) solutions. Also plotted are some of the single-energy phase shifts reported by many investigators (Ref. 2). (a) S_{11} phase shifts. (b) S_{31} phase shifts. (c) P_{11} phase shifts. (d) P_{31} phase shifts. (e) P_{13} phase shifts. (f) P_{33} phase shifts.

behavior used for the absorption parameters would be incorrect for a state in which the first important inelastic process has a final orbital angular momentum different from the initial angular momentum. For example,

$$\pi+p\rightarrow \mathrm{ABC}+n$$

would be such a process, where ABC is a 0^{++} meson with isospin 0. The final state is a pure $T=\frac{1}{2}$ state. Thus the P_{11} initial state would be responsible for producing an S-wave final state, and the threshold behavior would be $k-k_0$ rather than $(k-k_0)^3$ for the P_{11} absorption parameter.

(2) Allowing all powers of k in the sums of Eqs. (4) and (5) does not give the usual analytic behavior. One would expect only even powers of k.[2] We tried fitting with even powers in the 0–350-MeV analysis, but found that we could get better fits using all powers.

(3) Satisfaction of the dispersion relation which connects the real and imaginary parts of the partial-wave amplitudes is not guaranteed. The Yale[6] and Rutherford[7] analyses have this feature built in.

Unexpectedly, the 0–350-MeV analysis yielded a P_{11} phase shift negative below 150 MeV, and large and positive at 350 MeV (32°). Upon extension of the analysis to 700 MeV, we are unable to get good fits to the data unless we allow the P_{11} phase shift to become large; indeed, the best fit occurs when the P_{11} resonates at approximately 585 MeV along with the D_{13} resonance at about 638 MeV. However, a comparable fit was obtained when we restricted the P_{11} phase shift to be less than 90° (see Table VI). The P_{11} phase must be large; the available data give slight indications that it goes through 90°.

In solution 14 of Table VI, our best fit, the main effect of the P_{11} phase shift is on the π-p differential cross section at the forward angles. Appreciable reduction of the P_{11} phase shift from the large values obtained causes the forward π-p cross section to fall far below the observed values throughout the 300–600-MeV energy region.

The 0–100-, 0–350-, and 0–700-MeV solutions appear consistent with each other in the large phases. No error bands have yet been obtained for these solutions, but work is underway to obtain an error matrix.

Investigations are planned to determine what kind of data are needed to establish more precisely the pion-nucleon phase shifts. Also, "modified" energy-dependent phase-shift analyses are planned in which the higher angular-momentum states ($l>l_m$) are accounted for by the nearest singularities in the $\cos\theta$ complex plane.[11,34] We are presently attempting to extend the analysis to 1100 MeV.

We have recently been informed of extensive single energy analyses from 310 to 700 MeV by Cence[35] and Auvil *et al.*[36] We plan to try to fit our parametrization to these single energy values and see how well they fit all of the data simultaneously. Since we are now in a position to test quickly proposed new solutions against the data, we remain open to proposals for different combinations of phases which might account for the observations.

[34] G. L. Kane and T. D. Spearman, Phys. Rev. Letters **11**, 45 (1963); G. L. Kane, Ph.D. thesis, University of Illinois, 1963 (unpublished).

ACKNOWLEDGMENTS

The authors (especially L.D.R.) are deeply indebted to Dr. Michael J. Moravcsik, who advised concerning, and arranged for, the computer calculations during the early stages of the analysis. Dr. Moravcsik also provided encouragement and much theoretical advice.

Richard A. Arndt developed most of the computation methods used in our analysis. One of us (R.M.W.) revised his methods for this particular case. His initial work and advice during later stages of the analysis are greatly appreciated. Also, Eldon J. Halda has contributed to the computer calculations.

Our gratitude is extended to many experimentalists who sent us preliminary data, especially to the Moyer group at Berkeley.

The computations were done at the Lawrence Radiation Laboratory Computing Center at Livermore. One of us (L.D.R.) wishes to thank Dr. Sidney Fernbach for granting him a Postdoctoral Appointment at Lawrence Radiation Laboratory, Livermore, and for providing the many hours of computer time necessary to carry out this analysis.

APPENDIX I: BASIC EQUATIONS

We list here the basic equations for pion-nucleon scattering in our notation.

Total Cross Section

$$\sigma_T=(4\pi\lambda\!\!\!^{-}/k)f(0)\,,$$

where $\lambda\!\!\!^{-}=\hbar/\mu c=1.4135\times10^{-13}$ cm and k is the incident pion c.m. momentum.

Differential Cross Section for Unpolarized Target

$$\sigma(\theta)=|f(\theta)|^2+|g(\theta)|^2\,,$$

where θ is the c.m. pion scattering angle.

Recoil-Nucleon Polarization for Unpolarized Target

$$P(\theta)=-2\,\mathrm{Im}[f^*(\theta)g(\theta)]\hat{n}/\sigma(\theta)\,,$$

where $\hat{n}=(\mathbf{k}\times\mathbf{k}')/|\mathbf{k}\times\mathbf{k}'|$ and $k'=$final pion c.m. momentum.

Differential Cross Section for Polarized Target

$$\sigma(\theta)=|f(\theta)|^2+|g(\theta)|^2-2\,\mathrm{Im}[f^*(\theta)g(\theta)](\hat{n}\cdot\mathbf{P}_i)\,.$$

[35] R. J. Cence, University of Hawaii (private communication).
[36] P. Auvil, A. Donnachie, A. T. Lea, and C. Lovelace, Phys. Letters **12**, 76 (1964).

Recoil-Nucleon Polarization for Polarized Target

$$\mathbf{P}_f(\theta)=\{-2\,\mathrm{Im}[f^*(\theta)g(\theta)]\hat{n}-2\,\mathrm{Re}[f^*(\theta)g(\theta)](\hat{n}\times\mathbf{P}_i)+(|f(\theta)|^2+|g(\theta)|^2)(\hat{n}\cdot\mathbf{P}_i)\hat{n}-(|f(\theta)|^2-|g(\theta)|^2)\times[\hat{n}\times(\hat{n}\times\mathbf{P}_i)]\}/\sigma(\theta),$$

where $\mathbf{P}_i$ is the initial polarization.

Nonspin-Flip Amplitude

$$f(\theta)=\frac{\lambda}{k}\sum_{l=0}^{l_m}[(l+1)A_{l+}+lA_{l-}]P_l(\cos\theta),$$

where l_m is the maximum value of the angular momentum l used in the analysis.

Spin-Flip Amplitude

$$g(\theta)=\frac{\lambda}{k}\sum_{l=0}^{l_m}[A_{l+}-A_{l-}]P_l^1(\cos\theta).$$

Partial-Wave Amplitude

$$A_{l\pm}=(1/2i)[\eta_{l\pm}\exp(2i\delta_{l\pm})-1],$$

where $\delta_{l\pm}$ is the phase shift and $\eta_{l\pm}$ is the absorption parameter for scattering in the states with $J=l\pm\frac{1}{2}$.

Observable Amplitudes in Terms of Isotopic Spin Amplitudes

$$A_{l\pm}{}^{+}=A_{l\pm}{}^{(3)},\quad A_{l\pm}{}^{-}=\tfrac{1}{3}(A_{l\pm}{}^{(3)}+2A_{l\pm}{}^{(1)}),$$

and

$$A_{l\pm}{}^{\mathrm{cx}}=\tfrac{1}{3}\sqrt{2}(A_{l\pm}{}^{(3)}-A_{l\pm}{}^{(1)}),$$

where the superscripts have the following meanings:

$+$: $\pi^+ + p \rightarrow \pi^+ + p$,

$-$: $\pi^- + p \rightarrow \pi^- + p$,

cx: $\pi^- + p \rightarrow \pi^0 + n$,

(3): $T=\frac{3}{2}$,

(1): $T=\frac{1}{2}$.

APPENDIX II: DATA REFERENCES

A. Total Cross-Section References

$1=\sigma_T{}^+$; $2=\sigma_T{}^-$.

A1. C. Chedester, P. Isaacs, A. Sachs, and J. Steinberger, Phys. Rev. **82**, 958 (L) (1951)—2.

A2. H. L. Anderson, E. Fermi, E. A. Long, R. Martin, and D. E. Nagle, Phys. Rev. **85**, 934 (L) (1952)—2.

A3. H. L. Anderson, E. Fermi, E. A. Long, and D. E. Nagle, Phys. Rev. **85**, 936 (L) (1952)—1.

A4. H. L. Anderson, E. Fermi, D. E. Nagle, and G. B. Yodh, Phys. Rev. **86**, 413 (1952)—1, 2.

A5. H. L. Anderson, E. Fermi, D. E. Nagle, and G. B. Yodh, Phys. Rev. **86**, 793 (L) (1952)—1.

A6. E. C. Fowler, W. B. Fowler, R. P. Shutt, A. M. Thorndike, and W. L. Whittemore, Phys. Rev. **86**, 1053 (L) (1952)—1.

A7. P. Isaacs, A. Sachs, and J. Steinberger, Phys. Rev. **85**, 803 (1953)—1, 2.

A8. G. Goldhaber, Phys. Rev. **89**, 1187 (1953)—1.

A9. H. L. Anderson, E. Fermi, R. Martin, and D. E. Nagle, Phys. Rev. **91**, 155 (1953)—1, 2.

A10. J. P. Perry and C. E. Angell, Phys. Rev. **91**, 1289 (L) (1953)—1.

A11. E. Fermi, M. Glicksman, R. Martin, and D. Nagle, Phys. Rev. **92**, 161 (1953)—2.

A12. W. B. Fowler, R. M. Lea, W. D. Shephard, R. P. Shutt, A. M. Thorndike, and W. L. Whittemore, Phys. Rev. **92**, 832 (L) (1953)—1.

A13. C. E. Angell and J. P. Perry, Phys. Rev. **92**, 835 (L) (1953)—1.

A14. A. M. Shapiro, C. P. Leavitt, and F. F. Chen, Phys. Rev. **92**, 1073 (L) (1953)—2.

A15. S. J. Lindenbaum and L. C. L. Yuan, Phys. Rev. **92**, 1578 (L) (1953)—2.

A16. R. L. Cool, L. Madansky, and O. Piccioni, Phys. Rev. **93**, 249 (L) (1954)—2.

A17. G. Homa, G. Goldhaber, and L. M. Lederman, Phys. Rev. **93**, 554 (1954)—1.

A18. S. L. Leonard and D. H. Stork, Phys. Rev. **93**, 568 (1954)—1.

A19. J. Orear, J. J. Lord, and A. B. Weaver, Phys. Rev. **93**, 575 (1954)—1.

A20. R. Cool, L. Madansky, and O. Piccioni, Phys. Rev. **93**, 637 (1954)—2.

A21. D. Bodansky, A. M. Sachs, and J. Steinberger, Phys. Rev. **93**, 1367 (1954)—1, 2.

A22. M. Glicksman, Phys. Rev. **94**, 1335 (1954)—1, 2.

A23. J. Orear, C. H. Tsao, J. J. Lord, and A. B. Weaver, Phys. Rev. **95**, 624 (1954)—1.

A24. M. Glicksman, Phys. Rev. **95**, 1045 (1954)—2.

A25. J. Ashkin, J. P. Blaser, F. Feiner, J. G. Gorman, and M. O. Stern, Phys. Rev. **96**, 1104 (1954)—1, 2.

A26. J. Orear, Phys. Rev. **96**, 1417 (1954)—1.

A27. S. J. Lindenbaum and L. C. L. Yuan, *Proceedings of the Fourth Annual Rochester Conference on High Energy Nuclear Physics* (University of Rochester Press, Rochester, 1954), p. 99—1, 2.

A28. R. A. Grandey and A. F. Clark, Phys. Rev. **97**, 791 (1955)—1.

A29. L. M. Eisberg, W. B. Fowler, R. M. Lea, W. D. Shephard, R. P. Shutt, A. M. Thorndike, and W. L. Whittemore, Phys. Rev. **97**, 797 (1955)—2.

A30. H. L. Anderson and M. Glicksman, Phys. Rev. **100**, 268 (1955)—1, 2.

A31. H. L. Anderson, W. C. Davidon, M. Glicksman, and U. E. Kruse, Phys. Rev. **100**, 279 (1955)—1, 2.

A32. S. J. Lindenbaum and L. C. L. Yuan, Phys. Rev. **100**, 306 (1955)—1.

A33. A. M. Sachs, H. Winick, and B. A. Wooten, Phys. Rev. **100**, 1255 (A) (1955)—1.

A34. A. E. Ignatenko, A. I. Mukhin, E. B. Ozerov, and B. M. Pontecorvo, Dokl. Akad. Nauk SSSR **103**, 45 (1955)—2.

A35. H. D. Taft, Phys. Rev. **101**, 1116 (1956)—1.

A36. J. Ashkin, J. P. Blaser, F. Feiner, and M. O. Stern, Phys. Rev. **101**, 1149 (1956)—1, 2.

A37. S. L. Whetstone, Jr. and D. H. Stork, Phys. Rev. **102**, 251 (1956)—1.

A38. R. Cool, O. Piccioni, and D. Clark, Phys. Rev. **103**, 1082 (1956)—1.

A39. W. H. Evans, CERN Symposium, 1956 (unpublished)—1.

A40. A. E. Ignatenko, A. I. Mukhin, E. B. Ozerov, and B. M. Pontecorvo, Zh. Eksperim. i Teor. Fiz. **30**, 7 (1956) [English transl.: Soviet Phys.—JETP **3**, 10 (1956-7)]—1.

A41. M. Kozodaev, R. Suliaev, A. Filippov, and Iu. Shcherbakov, Dokl. Akad. Nauk SSSR **107**, 236 (1956) [English transl.: Soviet Phys.—Doklady **1**, 171 (1956)]—2.

A42. L. S. Dul'kova, J. B. Sokolova, and M. I. Shafranova, Dokl. Akad. Nauk SSSR **111**, 992 (1956) [English transl.: Soviet Phys.—Doklady **1**, 739 (1956)]—1, 2.

A43. J. Ashkin, J. P. Blaser, F. Feiner, and M. O. Stern, Phys. Rev. **105**, 724 (1957)—1, 2.

A44. G. Ferrari, E. Manaresi, and G. Quareni, Nuovo Cimento **5**, 1651 (1957)—1.

A45. R. Gessaroli, G. Quareni, G. Dascoli, S. Mora, and G. Todesco, Nuovo Cimento **5**, 1658 (1957)—1.

A46. L. Ferretti, G. Quareni, M. Della-Corte, and T. Fazzini, Nuovo Cimento **5**, 1660 (1957)—1.

A47. A. I. Mukhin, E. B. Ozerov, and B. M. Pontecorvo, Zh. Eksperim. i Teor. Fiz. **31**, 371 (1956) [English transl.: Soviet Phys.—JETP **4**, 237 (1957)]—1.
A48. A. M. Sachs, H. Winick, and B. A. Wooten, Phys. Rev. **109**, 1750 (1958)—1.
A49. S. J. Lindenbaum and L. C. L. Yuan, Phys. Rev. **111**, 1380 (1958)—1.
A50. V. I. Zinov and S. M. Korenchenko, Zh. Eksperim. i Teor. Fiz. **33**, 1307 (1957) [English transl.: Soviet Phys.—JETP **6**, 1006 (1958)]—2.
A51. V. I. Zinov and S. M. Korenchenko, Zh. Eksperim. i Teor. Fiz. **33**, 1308 (1957) [English transl.: Soviet Phys.—JETP **6**, 1007 (1958)]—2.
A52. W. B. Johnson and M. Camac, Bull. Am. Phys. Soc. **3**, 197 (1958)—1.
A53. B. McCormick and L. Baggett, CERN Symposium, 1958 (unpublished)—2.
A54. G. E. Fischer and E. M. Jenkins, Phys. Rev. **116**, 749 (1959)—1.
A55. W. J. Willis, Phys. Rev. **116**, 753 (1959)—1.
A56. U. E. Kruse and R. C. Arnold, Phys. Rev. **116**, 1008 (1959)—2.
A57. V. Alles-Borelli, S. Bergia, E. Perez-Ferreira, and P. Waloschek, Nuovo Cimento **14**, 211 (1959)—2.
A58. V. G. Zinov and S. M. Korenchenko, Zh. Eksperim. i Teor. Fiz. **36**, 618 (1959) [English transl.: Soviet Phys.—JETP **9**, 429 (1959)]—2.
A59. D. N. Edwards, S. G. F. Frank, and J. R. Holt, Proc. Phys. Soc. (London) **73**, 856 (1959)—2.
A60. I. Derado, G. Lütjens, and N. Schmitz, Am. Phys. Leipzig **4**, 103 (1959)—2.
A61. H. C. Burrowes, D. O. Caldwell, D. H. Frisch, D. A. Hill, D. M. Ritson, R. A. Schluter, and M. A. Wahlig, Phys. Rev. Letters **2**, 119 (1959)—1.
A62. R. R. Crittenden, J. H. Scandrett, W. D. Shephard, W. D. Walker, and J. Ballam, Phys. Rev. Letters **2**, 121 (1959)—2.
A63. A. Loria, P. Mittner, R. Santengelo, G. Zago, A. Brenner, J. L. Montonet, *Proceedings of the Ninth Annual International Conference on High Energy Physics*, Kiev, 1959 (Academy of Science, USSR, 1960)—1.
A64. D. Miller and J. Ring, Phys. Rev. **117**, 582 (1960)—1.
A65. D. N. Edwards, S. G. F. Frank, and J. R. Holt [quoted in H. P. Noyes and D. N. Edwards, Phys. Rev. **118**, 1409 (1960)]—1.
A66. V. G. Zinov, A. D. Konin, S. M. Korenchenko, and B. Pontecorvo, Zh. Eksperim. i Teor. Fiz. **38**, 1708 (1960) [English transl.: Soviet Phys.—JETP **11**, 1233 (1960)]—2.
A67. D. Radojiico, cited by R. F. Peierls, Phys. Rev. Letters **5**, 166 (1960)—2.
A68. N. P. Klepikov, V. A. Meshcheryakov, and S. N. Sokolov, Joint Institute of Nuclear Research Report JINR-D-584, 1960 (compilation) (unpublished).
A69. M. Derrick, I. Fetkovich, T. Fields, E. G. Pewett, and G. B. Yodh, *Proceedings of the Tenth Annual International Conference on High Energy Physics, Rochester* (Interscience Publishers, Inc., New York, 1960)—2.
A70. S. Barnes, B. Rose, G. Giacomelli, J. Ring, and K. Miyake, Phys. Rev. **117**, 226 (1960)—1, 2.
A71. J. C. Caris, L. K. Goodwin, R. W. Kenney, V. Perez-Mendez, and W. A. Perkins, III, Phys. Rev. **122**, 262 (1961)—2.
A72. J. H. Foote, O. Chamberlain, E. H. Rogers, and H. M. Steiner, Phys. Rev. **122**, 959 (1961)—1.
A73. J. Deahl, M. Derrick, J. Fetovich, T. Fields, and G. B. Yodh, Phys. Rev. **124**, 1987 (1961)—2.
A74. J. C. Brisson, J. F. Detoeuf, P. Falk-Vairant, L. Van-Rossum, and G. Valladas, Nuovo Cimento **19**, 210 (1961)—1, 2.
A75. V. S. Barashenkov and V. M. Maltsev, Fortschr. Physik **9**, 549 (1961) (compilation).
A76. R. I. Salukvadse and D. Nyagu, Joint Institute of Nuclear Research Report JINR-P-671, 1961 (unpublished)—1, 2.
A77. J. K. Kopp, A. M. Shapiro, R. I. Island, and A. R. Erwin, Phys. Rev. Letters **6**, 327 (1961)—1.
A78. K. Miyake, K. F. Kinsey, and D. E. Knapp, Bull. Am. Phys. Soc. **6**, 311 (1961)—2.
A79. H. Foelsche, E. C. Fowler, H. L. Kraybill, J. R. Sanford, and D. Stonehill, *International Conference on High Energy Nuclear Physics, Geneva, 1962*, edited by J. Prentki (CERN Scientific Information Service, Geneva, Switzerland, 1962)—1.
A80. T. J. Devlin, B. J. Moyer, and V. Perez-Mendez, Phys. Rev. **125**, 690 (1962)—1, 2.
A81. M. J. Longo and B. J. Moyer, Phys. Rev. **125**, 701 (1962)—1.
A82. H. R. Rugge and O. T. Vik, Phys. Rev. **129**, 2300 (1963)—2.
A83. S. Kellman, W. P. Kovacik, and T. A. Romanowski, Phys. Rev. **129**, 365 (1963)—2.
A84. Saclay-Orsay-Bari-Bologna collaboration, Nuovo Cimento **29**, 515 (1963)—2.

B. Differential-Cross-Section References

$3=\sigma^{+}(\theta)$; $4=\sigma^{-}(\theta)$; $5=\sigma^{ex}(\theta)$.

B1. H. L. Anderson, E. Fermi, D. E. Nagle, and G. B. Yodh, Phys. Rev. **86**, 793 (L) (1952)—5.
B2. E. C. Fowler, W. B. Fowler, R. P. Shutt, A. M. Thorndike, and W. L. Whittemore, Phys. Rev. **86**, 1053 (L) (1952)—3.
B3. G. Goldhaber, Phys. Rev. **89**, 1187 (1953)—3.
B4. H. L. Anderson, E. Fermi, R. Martin, and D. E. Nagle, Phys. Rev. **91**, 155 (1953)—3, 4, 5.
B5. J. P. Perry and C. E. Angell, Phys. Rev. **91**, 1289 (L) (1953)—3.
B6. J. Orear, Phys. Rev. **92**, 156 (1953)—4.
B7. E. Fermi, M. Glicksman, R. Martin, and D. Nagle, Phys. Rev. **92**, 161 (1953)—4, 5.
B8. W. B. Fowler, R. M. Lea, W. D. Shephard, R. P. Shutt, A. M. Thorndike, and W. L. Whittemore, Phys. Rev. **92**, 832 (L) (1953)—3.
B9. G. Homa, G. Goldhaber, and L. M. Lederman, Phys. Rev. **93**, 554 (1954)—3.
B10. J. Orear, J. J. Lord, and A. B. Weaver, Phys. Rev. **93**, 575 (1954)—3.
B11. D. Bodansky, A. M. Sachs, and J. Steinberger, Phys. Rev. **93**, 918 (A) (1954)—5.
B12. D. Bodansky, A. M. Sachs, and J. Steinberger, Phys. Rev. **93**, 1367 (1954)—3, 4, 5.
B13. M. Glicksman, Phys. Rev. **94**, 1335 (1954)—4, 5.
B14. J. Tinlot and A. Roberts, Phys. Rev. **95**, 137 (1954)—5.
B14a. J. Orear, C. H. Tsao, J. J. Lord, and A. B. Weaver, Phys. Rev. **95**, 624 (A) (1954)—3.
B15. M. Glicksman, Phys. Rev. **95**, 1045 (1954)—5.
B16. J. Orear, Phys. Rev. **96**, 1417 (1954)—3.
B17. R. A. Grandey and A. F. Clark, Phys. Rev. **97**, 791 (1953)—3.
B18. L. M. Eisberg, W. B. Fowler, R. M. Lea, W. D. Shephard, R. P. Shutt, A. M. Thorndike, and W. L. Whittemore, Phys. Rev. **97**, 797 (1955)—4.
B19. H. L. Anderson and M. Glicksman, Phys. Rev. **100**, 268 (1955)—3, 4, 5.
B20. H. L. Anderson, W. C. Davidon, M. Glicksman, and U. E. Kruse, Phys. Rev. **100**, 279 (1955)—3, 4, 5.
B21. L. Ferretti, E. Manaressi, G. Puppi, and A. Ranzi, Nuovo Cimento **1**, 1238 (1955)—3.
B22. H. D. Taft, Phys. Rev. **101**, 1116 (1956)—3.
B23. J. Ashkin, J. P. Blaser, F. Feiner, and M. O. Stern, Phys. Rev. **101**, 1149 (1956)—3, 4, 5.
B24. S. L. Whetstone, Jr. and D. H. Stork, Phys. Rev. **102**, 251 (1956)—3.
B25. W. D. Walker, F. Hushfar, and W. D. Shephard, Phys. Rev. **104**, 526 (1956)—4.
B26. L. S. Dul'kova, I. A. Romanova, I. B. Sokolova, L. V. Sukhov, K. D. Tolstov, and M. G. Shafronova, Dokl. Akad. Nauk SSSR **107**, 43 (1956)[English transl.: Soviet Phys.—Doklady **1**, 154 (1956)]—4.
B27. M. Kozodaev, R. Suliaev, A. Fillippov, and Iu. Shcherbakov, Dokl. Akad. Nauk SSSR **107**, 236 (1956) [English transl.: Soviet Phys.—Doklady **1**, 171 (1956)]—4.
B28. L. S. Dul'kova, I. B. Sokolova, and M. G. Shafronova, Dokl. Akad. Nauk SSSR **111**, 992 (1957) [English transl.: Soviet Phys.—Doklady **1**, 739 (1956)]—3, 4.
B29. G. Ferrari, L. Ferretti, R. Gessaroli, E. Manaressi, G. Puppi, G. Quareni, A. Ranzi, and A. Stanghellini, *Proceedings of the CERN Symposium on High-Energy Accelerators and Pion Physics, Geneva, 1956* (CERN Scientific Information Service, Geneva, 1956), p. 230—3.
B30. J. Ashkin, J. P. Blaser, F. Feiner, and M. O. Stern, Phys. Rev. **105**, 724 (1957)—3, 4, 5.

B31. M. Chretien, J. Leitner, N. P. Samios, M. Schwartz, and J. Steinberger, Phys. Rev. **108**, 383 (1957)—4.
B32. G. Ferrari, E. Manaressi, and G. Quareni, Nuovo Cimento **5**, 1651 (1957)—3.
B33. R. Gessaroli, G. Quareni, G. Dascoli, S. Mora, and G. Todesco, Nuovo Cimento **5**, 1658 (1957)—3.
B34. L. Ferretti, G. Quareni, M. Della-Corte, and T. Fazzini, Nuovo Cimento **5**, 1660 (1957)—3.
B35. A. I. Mukhin, E. B. Ozerov, and B. M. Pontecorvo, Zh. Eksperim. i Teor. Fiz. **31**, 371 (1956) [English transl.: Soviet Phys.—JETP **4**, 237 (1957)]—3.
B36. N. A. Mitin and E. L. Grigor'ev, Zh. Eksperim. i Teor. Fiz. **32**, 445 (1957) [English transl.: Soviet Phys.—JETP **5**, 378 (1957)]—3.
B37. A. R. Erwin, Jr. and J. K. Kopp, Phys. Rev. **109**, 1364 (1958)—4.
B38. A. M. Sachs, H. Winick, and B. A. Wooten, Phys. Rev. **109**, 1750 (1958)—3.
B39. M. E. Blevins, M. M. Block, and J. Leitner, Phys. Rev. **112**, 1287 (1958)—3.
B40. L. Baggett, Lawrence Radiation Laboratory (Berkeley) Report UCRL-8302, 1958 (unpublished)—4.
B41. E. Garwin, K. Kernan, C. O. Kin, and C. M. York, Phys. Rev. **115**, 1295 (1959)—5.
B42. W. J. Willis, Phys. Rev. **116**, 753 (1959)—3.
B43. L. O. Roellig and D. A. Glaser, Phys. Rev. **116**, 1001 (1959)—3.
B44. U. E. Kruse and R. C. Arnold, Phys. Rev. **116**, 1008 (1959)—4.
B45. D. N. Edwards, S. G. F. Frank, and J. R. Holt, Proc. Phys. Soc. (London) **73**, 856 (1959)—4.
B46. R. R. Crittenden, J. H. Scandrett, W. D. Shephard, W. D. Walker, and J. Ballam, Phys. Rev. Letters **2**, 121 (1959)—4.
B47. S. W. Barnes, B. Rose, G. Giacomelli, J. Ring, K. Miyake, and K. Kinsey, Phys. Rev. **117**, 226 and 238 (1960)—4.
B48. G. Giacomelli, Phys. Rev. **117**, 250 (1960)—3, 4.
B49. D. Miller and J. Ring, Phys. Rev. **117**, 582 (1960)—3.
B50. I. Derado and N. Schmitz, Phys. Rev. **118**, 309 (1960)—4.
B51. W. J. Kernan, Phys. Rev. **119**, 1092 (1960)—5.
B52. C. M. York, W. J. Kernan, and E. L. Garwin, Phys. Rev. **119**, 1096 (1960)—5.
B53. S. Bergia, L. Bertocchi, V. Borelli, G. Brautti, L. Chersovanni, L. Lavatelli, A. Minguzzi-Ranzi, R. Tosi, P. Waloschek, and V. Zoboli, Nuovo Cimento **15**, 551 (1960)—4.
B54. E. L. Grigor'ev and N. A. Mitin, Zh. Eksperim. i Teor. Fiz. **37**, 1583 (1959)[English transl.: Soviet Phys.—JETP **10**, 1123 (1960)]—3.
B55. I. M. Vasilevskii and V. V. Vishnyakov, Zh. Eksperim. i Teor. Fiz. **38**, 441 (1960) [English transl.: Soviet Phys.—JETP **11**, 323 (1960)]—4.
B56. Yu. A. Budagov, S. Wiktov, V. P. Dzelepov, P. F. Ermolov, and V. I. Moskalev, Zh. Eksperim. i Teor. Fiz. **38**, 734 (1960) [English transl.: Soviet Phys.—JETP **11**, 531 (1960)]—4.
B57. V. G. Zinov and S. M. Korenchenko, Zh. Eksperim. i Teor. Fiz. **38**, 1099 (1960) [English transl.: Soviet Phys.—JETP **11**, 794 (1960)]—4.
B58. V. G. Zinov and S. M. Korenchenko, Zh. Eksperim. i Teor. Fiz. **38**, 1399 (1960) [English transl.: Soviet Phys.—JETP **11**, 1010 (1960)]—5.
B59. J. C. Caris, R. W. Kenney, V. Perez-Mendez, and W. A. Perkins, III, Phys. Rev. **121**, 893 (1961)—5.
B60. L. K. Goodwin, R. W. Kenney, and V. Perez-Mendez, Phys. Rev. **122**, 655 (1961)—4.
B61. J. H. Foote, O. Chamberlain, E. H. Rogers, and H. M. Steiner, Phys. Rev. **122**, 959 (1961)—3.
B62. J. K. Kopp, A. M. Shapiro, and A. R. Erwin, Phys. Rev. **123**, 301 (1961)—3.
B63. B. C. Maglić, B. T. Feld, and C. A. Diffey, Phys. Rev. **123**, 1444 (1961)—4.
B64. J. Deahl, M. Derrick, J. Fetkovich, T. Fields, and G. B. Yodh, Phys. Rev. **124**, 1987 (1961)—4.
B65. L. Bertanzi, R. Carrara, A. Drago, P. Franzini, I. Mannelli, G. V. Silvestrini, and P. H. Stoker, Nuovo Cimento **19**, 467 (1961)—4.
B66. F. Grard, G. MacLeod, L. Montanet, M. Cresti, R. Barloutaud, C. Choquet, J. Gaillard, J. Heughebaert, A. Leveque, P. Lehmann, J. Meyer, and D. Revel, Nuovo Cimento **22**, 193 (1961)—4.
B67. A. Loria, P. Mittner, E. Santangello, I. Scotani, G. Zogo, B. Aubert, A. Brenner, Y. Goldschmidt-Clermont, F. Grard, G. MacLeod, A. Minguzzi-Ranzi, and L. Montanet, Nuovo Cimento **22**, 820 (1961)—3.
B68. C. D. Wood, T. J. Devlin, J. A. Helland, M. J. Longo, B. J. Moyer, and V. Perez-Mendez, Phys. Rev. Letters **6**, 481 (1961)—4.
B69. K. W. Lai, L. W. Jones, and M. L. Perl, Phys. Rev. Letters **7**, 125 (1961)—4.
B70. K. Miyake, K. F. Kinsey, and D. E. Knapp, Phys. Rev. **126**, 2188 (1962)—5.
B71. U. Bidan, F. Lévy, N. Abbattista, A. Minafra, S. Mongelli, A. Romano, and P. Waloschek, Nuovo Cimento **24**, 334 (1962)—3.
B72. R. Barloutaud, C. Choquet-Loudec, A. Derem, J. Heughebaert, A. Leveque, and J. Meyer, Phys. Letters **1**, 207 (1962)—3.
B73. R. Barloutaud, L. Cardin, A. Deren, C. Gensollen, A Leveque, C. Louedec, J. Meyer, and D. Tycho, Nuovo Cimento **26**, 1409 (1962)—3.
B74. H. R. Rugge and O. T. Vik, Phys. Rev. **129**, 2300 (1963)—4.
B75. V. Cook, B. Cork, W. R. Holley, and M. L. Perl, Phys. Rev. **130**, 762 (1963)—3.
B76. J. A. Helland, T. J. Devlin, D. E. Hagge, M. J. Longo, B. J. Moyer, and C. D. Wood, Lawrence Radiation Laboratory (Berkeley) Report UCRL-10478, 1962 (unpublished)—3, 4.
B77. S. Kellman, W. P. Kovacik, and T. A. Romanowski, Phys. Rev. **129**, 365 (1963)—4.
B78. M. Chretien, F. Bulos, H. R. Crouch, Jr., R. E. Lanou, Jr. *et al.*, Brookhaven National Laboratory (unpublished)—5.
B79. P. C. A. Newcomb, Lawrence Radiation Laboratory (Berkeley) Report UCRL-10682, 1963 (unpublished)—3.
B80. D. T. Massam (private communication)—3.
B81. G. Myatt (private communication, to be published)—5.
B82. D. E. Knapp and K. Kinsey, Phys. Rev. **131**, 1822 (1963) —3, 4.
B83. E. D. Alyea, Jr. (private communication)—3.
B84. Sacaly-Orsay-Bari-Bologna collaboration, Nuovo Cimento **29**, 515 (1963)—4.
B85. B. R. Riley (private communication)—4.
B86. J. I. Shonle, Phys. Rev. Letters **5**, 56 (1960) [superseded by Lawrence Radiation Laboratory (Berkeley) Report UCRL-9362 as revised by UC-34, 1961 (unpublished)]—4.
B87. G. Valladas, Saclay preprint, 1963 (unpublished)—3, 4.
B88. C. Chiu (private communication)—5.
B89. P. Ogden, Lawrence Radiation Laboratory (Berkeley) Report UCRL-11180, 1964 (unpublished)—3, 4.
B90. G. Yodh (private communication)—4.
B91. R. Kurtz and D. Lind, Lawrence Radiation Laboratory (Berkeley) Report UCRL-11548, 1964 (unpublished)—5.
B92. A. Muller, E. Pauli, R. Barloutoud, J. Meyer, M. Beneventano, G. Gialanella, and L. Paoluzi, Saclay Report LPCHE 64-11, 1964 (unpublished)—4.
B93. W. K. Troka, Lawrence Radiation Laboratory (Berkeley) Report UCRL-11537, 1964 (unpublished)—3.

C. Recoil-Nucleon Polarization References

$6=P^{+}(\theta)$; $7=P^{-}(\theta)$; $8=P^{\mathrm{ex}}(\theta)$.

C1. J. F. Kunze, T. A. Romanowski, J. Ashkin, and A. Burger, Phys. Rev. **117**, 895 (1960)—7.
C2. E. L. Grigor'ev and N. A. Mitin, Zh. Eksperim. i Teor. Fiz. **37**, 413 (1959) [English transl.: Soviet Phys.—JETP **10**, 295 (1960)]—6.
C3. I. M. Vasilevskii and V. V. Vishnyakov, Zh. Eksperim. i Teor. Fiz. **38**, 1644 (1960) [English transl.: Soviet Phys.—JETP **11**, 1185 (1960)] [superseded by Joint Institute of Nuclear Research Report JINR-D-1202, 1963 (unpublished)]—7.
C4. J. H. Foote, O. Chamberlain, E. H. Rogers, H. M. Steiner, C. E. Wiegand, and I. Ypsilantis, Phys. Rev. **122**, 948 (1961)—6.
C5. E. F. Beall, B. Cork, P. G. Murphy, W. A. Wentzel, C. M. P. Johnson, and L. J. Koester, Jr., Phys. Rev. **126**, 1554 (1962)—7.

C6. H. R. Rugge and O. T. Vik, Phys. Rev. **129**, 2300 (1963)—7.
C7. R. E. Hill, N. E. Booth, R. J. Esterling, D. L. Jenkins, N. H. Lipman, H. R. Rugge, and O. T. Vik, Bull. Am. Phys. Soc. **9**, 410 (1964) [superseded by R. E. Hill (private communication)]—8.
C8. R. D. Eandi, T. J. Devlin, P. G. McManigal, and B. J. Moyer, Phys. Rev. **136**, B536 (1964)—6, 7.
C9. O. Chamberlain, C. D. Jeffries, C. H. Schultz, G. Shapiro, and L. Van Rossum, Phys. Letters **7**, 293 (1963) [superseded by C. Schultz, Lawrence Radiation Laboratory (Berkeley) Report UCRL-11149, 1964 (unpublished)]—6.

PHYSICAL REVIEW VOLUME 138, NUMBER 1B 12 APRIL 1965

Nuclear Recoil in the Decay of Bound Muons; A Possible Tool in Muonic-Atom Studies

RICHARD M. WEINER
Labirint 28, Bucharest, Rumania
(Received 27 October 1964)

The nuclear-recoil spectrum in the decay of a bound muon is calculated using sudden perturbation theory and with neglect of the final Coulomb interaction between the μ-decay electron and the nucleus and of relativistic corrections to the muon wave function. In this approximation the recoil momentum distribution is identical with the square of the Bessel-Hankel transform of the bound muon wave function. By measuring the recoil spectrum one could gain important information about the muonic atom.

INTRODUCTION

THE muon, besides its intrinsic interest as an elementary particle, is also an important tool in nuclear and atomic physics. Due to the relatively large mass of the muon compared to that of the electron, the atomic system nucleus+muon has a radius more than 200 times smaller than the system nucleus+electron. That is why muonic atoms are very sensitive to the nuclear charge distribution and why muonic molecules can be formed which lead to fusion reactions with the muon playing the role of a catalyst which reduces the Coulomb potential barrier.

These facts, among others, explain the great interest in muonic atoms and molecules and the increasing number of works, both theoretical and experimental, dedicated to this subject.

Up to the present, information about muonic atoms has been gained by measuring the energies of the x and γ rays emitted in atomic transitions. However, this information is limited for several reasons:

(1) The energy does not specify completely the bound state of the muon.
(2) One measures only energy differences.
(3) The measured x-ray yields are still in disagreement with the theoretical predictions,[1] especially at low Z.

Some progress concerning item (1) has been achieved recently with the discovery of the hyperfine-structure effect in the nuclear capture of muons, but the information yielded by this effect (the relative spin orientation of the muon and the nucleus) is also limited.

Therefore a method which could offer more complete information about the bound states of the muon and about the corresponding absolute energy values would be highly desirable.

As to muonic molecules in nuclear reactions it would be very important to know what happens to the muon after the nuclear reaction, i.e., if and in what system it remains bound before decaying.

It is the purpose of this note to suggest a method which might in the near future, with the muon beam intensities available from meson factories, contribute to the solution of the problems mentioned above.

In atomic physics absolute energy levels are measured in ionization processes. With muonic atoms, because of the instability of these systems and the low intensities of muonic beams, such experiments are at present, and in the foreseeable future, impossible. However, we will show that the radioactive character of the muon is just the feature which opens up new possibilities in this field.

Quantum mechanics tells us that the most complete information about a state is given by the wave function (w.f.), with the aid of which all the characteristics of the state, including its energy, can be calculated.

In the following we want to suggest a possible method for the direct experimental determination of the squared wave function of a bound muon. This method would consist in the measurement of the momentum distribution of the nuclei recoiling in the decay of bound muons. This distribution is closely related to the muon w.f. in the bound state from which it decays. For light nuclei the recoil distribution is practically identical with the momentum distribution of the muon in the Bohr orbit. Only muons could be studied in this way. For mesons like π and K mesons, the nuclear capture process predominates even at low Z.

[1] Y. Eisenberg and D. Kessler, Phys. Rev. **130**, 2349 (1963).